Available online at www.sciencedirect.com
SCIENCE DIRECT®
Icarus 168 (2004) 344–366
ICARUS
www.elsevier.com/locate/icarus

Laboratory experiments of Titan tholin formed in cold plasma at various pressures: implications for nitrogen-containing polycyclic aromatic compounds in Titan haze

Hiroshi Imanaka,[a,b,*] Bishun N. Khare,[a] Jamie E. Elsila,[c] Emma L.O. Bakes,[a] Christopher P. McKay,[d] Dale P. Cruikshank,[d] Seiji Sugita,[b] Takafumi Matsui,[e] and Richard N. Zare [c]

[a] *SETI Institute/NASA Ames Research Center, MS239-11 NASA Ames Research Center, Moffett Field, CA 94035-1000, USA*
[b] *Department of Earth and Planetary Science, University of Tokyo, Japan*
[c] *Department of Chemistry, Stanford University, Stanford, CA 94305-5080, USA*
[d] *NASA Ames Research Center, Moffett Field, CA 94035-1000, USA*
[e] *Department of Complexity Science and Engineering, University of Tokyo, Japan*

Received 7 August 2003; revised 11 December 2003

Abstract

Titan, the largest satellite of Saturn, has a thick nitrogen/methane atmosphere with a thick global organic haze. A laboratory analogue of Titan's haze, called tholin, was formed in an inductively coupled plasma from nitrogen/methane = 90/10 gas mixture at various pressures ranging from 13 to 2300 Pa. Chemical and optical properties of the resulting tholin depend on the deposition pressure in cold plasma. Structural analyses by IR and UV/VIS spectroscopy, microprobe laser desorption/ionization mass spectrometry, and Raman spectroscopy suggest that larger amounts of aromatic ring structures with larger cluster size are formed at lower pressures (13 and 26 Pa) than at higher pressures (160 and 2300 Pa). Nitrogen is more likely to incorporate into carbon networks in tholins formed at lower pressures, while nitrogen is bonded as terminal groups at higher pressures. Elemental analysis reveals that the carbon/nitrogen ratio in tholins increases from 1.5–2 at lower pressures to 3 at 2300 Pa. The increase in the aromatic compounds and the decrease in C/N ratio in tholin formed at low pressures indicate the presence of the nitrogen-containing polycyclic aromatic compounds in tholin formed at low pressures. Tholin formed at high pressure (2300 Pa) consists of a polymer-like branched chain structure terminated with $–CH_3$, $–NH_2$, and $–C{\equiv}N$ with few aromatic compounds. Reddish-brown tholin films formed at low pressures (13–26 Pa) shows stronger absorptions (almost 10 times larger k-value) in the UV/VIS range than the yellowish tholin films formed at high pressures (160 and 2300 Pa). The tholins formed at low pressures may be better representations of Titan's haze than those formed at high pressures, because the optical properties of tholin formed at low pressures agree well with that of Khare et al. (1984a, Icarus 60, 127–137), which have been shown to account for Titan's observed geometric albedo. Thus, the nitrogen-containing polycyclic aromatic compounds we find in tholin formed at low pressure may be present in Titan's haze. These aromatic compounds may have a significant influence on the thermal structure and complex organic chemistry in Titan's atmosphere, because they are efficient absorbers of UV radiation and efficient charge exchange intermediaries. Our results also indicate that the haze layers at various altitudes might have different chemical and optical properties.

Keywords: Titan; Haze; Tholin; Spectroscopy; Organic chemistry; Nitrogen-containing polycyclic aromatic compounds

1. Introduction

Titan, the largest satellite of Saturn, has a thick atmosphere composed primarily of nitrogen and methane. The surface pressure is ∼ 1.5 bar, and the temperature at the surface is 94 K (Samuelson et al., 1981; Lindal et al., 1983). The existence of trace organic compounds, revealed by the Voyager IRIS instrument (Hanel et al., 1981, 1982; Kunde et al., 1981; Maguire et al., 1981) indicates that an active organic chemistry occurs in Titan's atmosphere (e.g., Yung et al., 1984; Thompson et al., 1991; Toublanc et al., 1995;

* Corresponding author.
E-mail address: himanaka@mail.arc.nasa.gov (H. Imanaka).

0019-1035/$ – see front matter
doi:10.1016/j.icarus.2003.12.014

Lara et al., 1996). This atmospheric photochemistry and radiation chemistry produces organic haze that is optically thick at visible wavelengths (e.g., Hunten et al., 1984). Above the main haze deck around 250 km altitudes, there is a thinner layer known as the detached haze between 300 and 400 km altitude (Smith et al., 1981, 1982a; Rages and Pollack, 1983) probably with distinct optical properties (Rannou et al., 2000). It is still unclear if the chemical compositions of the haze materials at high altitudes, particularly the detached haze, are different from that of the main haze lower in the atmosphere (McKay et al., 2001).

Laboratory simulations of Titan's atmosphere have been able to produce solid organic material, termed tholin, with the optical properties necessary to match the spectrum of Titan (Khare et al., 1984a; McKay et al., 1989). Tholin contains a variety of hydrocarbons and nitrogen compounds, including one to two-ring aromatics compounds, which were revealed by pyrolysis gas chromatography and mass spectrometry (Py-GC/MS) (Khare et al., 1984b; Ehrenfreund et al., 1995). It was shown by two-step laser desorption/multiphoton ionization mass spectrometry that tholin also contains a trace amount of polycyclic aromatic hydrocarbons (PAHs), which consist of a range of two to four-ring compounds (Sagan et al., 1993). The aromatic ring compounds were observed to form within the first 10 seconds of a RF discharge in CH_4/N_2 gas mixture (Khare et al., 2002).

The presence of aromatic macromolecules in Titan's haze has significant implications for its atmosphere. Aromatics can absorb UV/VIS light much more efficiently than most aliphatic hydrocarbons, because of their delocalized π electrons. Consequently both size and abundance of aromatic structures in haze may control the optical properties of haze, thus dominating the thermal structure of Titan's atmosphere. Recently, Bakes et al., (2002, 2003) has proposed that the charging of aromatic macromolecules has significant effects on the aerosol agglomeration processes and the chemistry occurring in the Titan's atmosphere.

However, it is controversial if Titan's haze contains a significant amount of aromatic macromolecules. Coll et al. (1999) could not find any aromatic compounds in tholin except benzene, while nitrogen-containing heteroaromatics and PAHs were detected previously (Khare et al., 1984b; Sagan et al., 1993; Ehrenfreund et al., 1995). Recent laboratory simulations have revealed that the optical properties and elemental compositions of tholins also depend on experimental conditions, such as the initial gas mixture and temperature (Sagan et al., 1984; Khare et al., 1984a; McDonald et al., 1994; McKay, 1996; Coll et al., 1995, 1999; Ramirez et al., 2002). However, it is not known what causes these differences. The variations of the aromatic structures can be one of the major differences in tholins formed under different experimental conditions.

To our knowledge, there has not been a systematic study of simulations carried out over the range of pressures that represent the production region of the haze on Titan. Therefore we have conducted a series of laboratory experiments forming Titan tholins at various deposition pressures. We have focused on the effects of deposition pressure in cold plasma on tholin production processes, since pressure is one of the key experimental parameters that control the plasma properties, such as electron/ion/radical densities, their collision frequencies and their kinetic energies. The resultant tholins were analyzed by various spectroscopic methods, such as IR spectroscopy, UV/VIS/NIR spectroscopy, microprobe laser desorption/ionization mass spectrometry, and Raman spectroscopy, focusing in particular on the amount and size of aromatics. We also conducted a combustion-based elemental analysis of the tholins. In the following sections we present these results and discuss the implications for the presence of the nitrogen-containing polycyclic aromatic compounds (N-PACs) in Titan's haze.

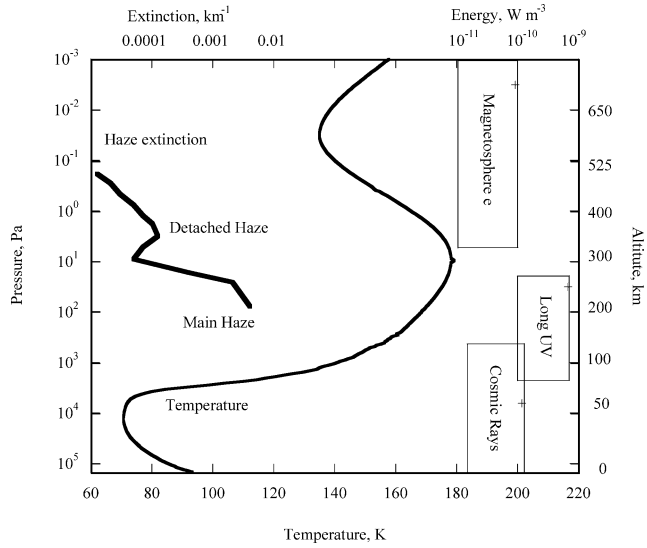

Fig. 1. Pressure and temperature of Titan's atmosphere (Yelle et al., 1997), showing the haze extinction (Rages and Pollack, 1983), and the available energy sources in Titan's atmosphere; saturnian magnetospheric electrons, long ultraviolet lights (> 155 nm), and cosmic rays (Sagan and Thompson, 1984; Sagan et al., 1992). The altitudes of maximum energy deposition are indicated by "+."

2. Experimental

In the upper atmosphere of Titan (> 300 km), both methane and nitrogen are dissociated by UV irradiation and the charged particle irradiation from the saturnian magnetosphere (Fig. 1). These dissociations ultimately lead to the formation of a lot of complex gas species and haze in Titan's atmosphere. In order to simulate these chemical reactions in high altitudes, we use a cold plasma inductively coupled with a RF power source. In contrast with a hot plasma, such as that produced by spark discharge or laser induced discharge, the temperature of the neutral gas in a cold plasma remains near room temperature even when the electron temperature is extremely high (e.g., Roth, 1995).

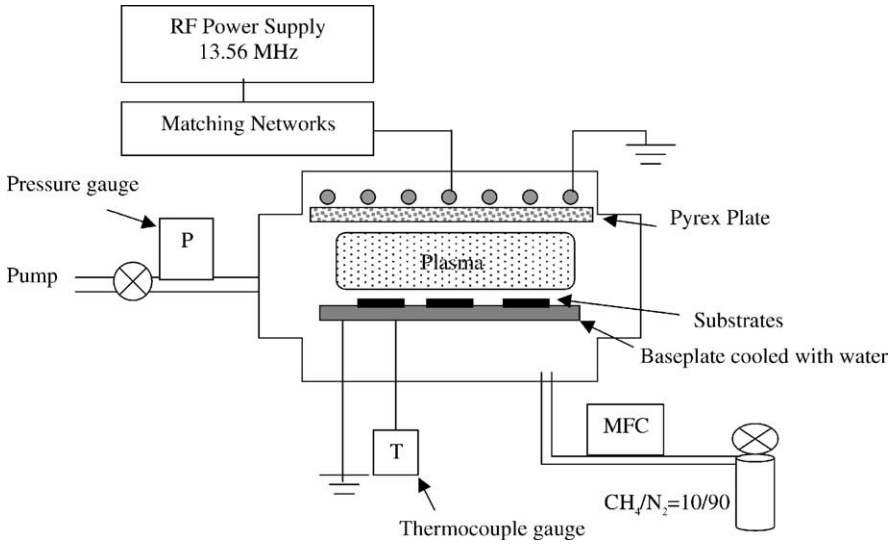

Fig. 2. Schematic of inductively coupled plasma reactor. A gas mixture of $CH_4/N_2 = 10/90$ was introduced by a mass flow controller (MFC).

While a hot plasma simulates lightning discharge or meteorite impact, a cold plasma more accurately simulates the charged particle irradiation by magnetospheric electrons and cosmic rays (Thompson et al., 1991). It is noticed that the cold plasma also emits a significant amount of UV light. In fact, most of the commercially available UV lamps use a glow discharge as the exciting source. Thus, the gas species in the plasma region are also irradiated with UV light. Although the quantitative ratio of the charged particle irradiation and UV irradiation in a cold plasma is not yet characterized well, we believe that a cold plasma simulates the full range of chemical reactions in Titan's upper atmosphere which are initiated by the dissociations of N_2 and CH_4 very well.

Figure 2 shows a schematic of the inductively coupled plasma (ICP) reactor consisting of a pair of electrodes mounted within a 25×25 cm stainless steel chamber. The two electrodes of 13 cm in diameter are placed 3 cm apart. The upper electrode consists of a six-turn copper coil that is inductively coupled to the plasma through a Pyrex coupling window. The lower electrode is grounded and cooled with water. The inductive coil is powered by a 13.56 MHz RF generator (Advanced Energy, RFX-600) with its associated custom matching networks. The forward and reflected powers are monitored by a power meter. Gases are fed and controlled by mass flow controllers (Tylan, 2900M). Pressure is measured with a capacitance gauge just downstream of the chamber. The temperature of the lower electrode is monitored by a thermocouple gauge. This parallel plate reactor is capable of both operating in a steady state and producing an uniform plasma over a diameter of 10 cm, typically with plasma densities of 10^{17} m^{-3} (Roth, 1995). The typical electron temperature is between a few eV and 10 eV (Lieberman and Lightenberg, 1994). These plasma parameters, however, depend in a complex way on the pressure, power, and geometry of the reactor.

Table 1
Experimental conditions

Pressure (Pa)	Flow rate (sccm[a])	Total time (hr)
13	9.6	1, 3, 5, 9
26	24	1, 3, 5, 8, 9
67	41	1, 5, 9
160	41	0.5, 1, 3, 8, 9
2300	41	0.5, 1, 3, 9

[a] sccm: standard cubic centimeter per minute.

In this study, pre-mixed $CH_4/N_2 = 10/90$ gas mixture (Matheson, CP grade) was introduced by a mass flow controller at a flow rate of 10–40 sccm (standard cubic centimeter per minute) to maintain the desired pressures. The power was kept at 100 W for all the experimental runs. The KBr, CaF_2, quartz, silicon, aluminum, and Pyrex glass substrates were placed on the lower electrode. Tholin was deposited on the substrates and formed at various pressures from 13 to 2300 Pa. Experimental conditions are listed in Table 1. More than 40 experimental runs were carried out. The temperature of the cooled base plate was always below 300 K during deposition, except for the experiment at 2300 Pa during which the plate temperature increased to 310 K. Thin films of tholin were removed from the chamber and were immediately measured by a FT–IR spectrometer (Nicolet, Nexus 670) and a UV/VIS/NIR spectrometer (Perkin Elmer, Lambda 900) in the ambient laboratory atmosphere. Further, thin films of tholin were analyzed by the dispersive Raman spectrometer (Nicolet, Almega 670) and by the microprobe laser-desorption, laser-ionization mass spectrometer (μL^2MS) at Stanford University. A few mg of tholin were collected by scratching and examined by conventional organic elemental analyzers (Thermo Quest 1100 NA at NASA Ames, and Perkin Elmer PE240 at Galbraith Lab. Inc., TN). Gas products were fractionally trapped in several cold traps of decreasing temperatures located downstream of

the chamber and analyzed by gas chromatography and mass spectrometer (GC/MS). During the plasma deposition, emission at UV/VIS wavelengths from the plasma region was monitored by a spectrometer (Ocean Optics, S2000) through the Pyrex window of the chamber. However, detailed analyses of gas products and UV/VIS emission lights are beyond the scope of this paper and will be published elsewhere.

The CH_4 abundance in Titan's lower stratosphere are in the range 1.5–3.4% (Lellouch et al., 1989) or even up to 4.4% (Courtin et al., 1995) and increases to $\sim$ 8% at 1125 km (Smith et al., 1982b). Recently, Lara et al. (2002) proposed the methane stratospheric mixing ratio up to 3.8% and placed the homopause at $\sim$ 1000 km, in order to fit to the observations of the methane thermospheric abundance (Smith et al., 1982b) and stratospheric mixing ratio of other minor constituents (Coustenis et al., 1989), although the precise CH_4 density profile is still not constrained very well (e.g., Strobel et al., 1992; Lara et al., 2002). In this study, we used $CH_4/N_2 = 10/90$ for initial gas mixture, which might be slightly larger abundance of CH_4 than in Titan's upper atmosphere. However, we found that the abundance of CH_4 in initial gas mixture was slightly reduced in the plasma region due to subsequent chemical reactions. In this study, however, we focused on the effect of pressure on the tholin properties and used the same gas composition that has been used in previous experimental work of the Cornell University Group (Khare et al., 1984a, 1984b, 1987; Thompson et al., 1991; Sagan et al., 1993). The effect of initial CH_4/N_2 ratio on the optical properties of tholin will be discussed in the future.

In Titan's upper atmosphere ($>$ 300 km) where both methane and nitrogen are dissociated, the chemical reaction occurs at low pressures less than $\sim$ 10 Pa (Sagan and Thompson, 1984). Generally, pressure is one of the key factors that determine the ratio of uni-, bi-, and trimolecular reactions, and thus may dominate the chemical properties of the reaction products. The lower pressure conditions in our cold plasma experiments (13 and 26 Pa) may correspond to the regions of Titan's upper atmosphere. The highest-pressure simulation (2300 Pa) may correspond to the radiation–chemical processes by cosmic rays at Titan's lower stratosphere around 75 km. In the stratosphere (100–300 km), further chemical reactions are induced by the catalytic CH_4 dissociation by such molecules as C_2H_2 and C_4H_2 absorbing the long UV ($>$ 155 nm) irradiation (Yung et al., 1984; Sagan and Thompson, 1984). These main absorbers of long UV irradiation in Titan's stratosphere are produced by the chemical reactions occurring in the upper atmosphere. (However, the energy deposition of long UV irradiation in the lower stratosphere would be overestimated below $\sim$ 200 km (Sagan and Thompson, 1984), because the shielding of the UV light by the overlaying haze was not considered, as Sagan and Thompson suggested in their paper. In fact, the dark UV albedo of Titan ($\sim$ 0.03) was explained by the UV absorption by the haze, thus overcoming the Rayleigh backscattering of gas molecules in the lower atmosphere (Courtin et al., 1991; Rannou et al., 1995).) Our cold plasma experiments at 67 and 160 Pa would partially simulate the photochemical processes in Titan's stratosphere because to the UV irradiation to the secondary gas products such as C_2H_2, although CH_4 and N_2 are also dissociated simultaneously in our experiments.

Saturnian magnetospheric electrons have a wide range of energy up to about 1 MeV (Krimigis et al., 1981, 1982; Vogt et al., 1981, 1982), and in Titan's atmosphere their energy deposition zone extends through several hundred kilometers of altitude from 300 km at $\sim$ 10 Pa to 1000 km at $\sim 10^{-4}$ Pa (Sagan and Thompson, 1984; Thompson et al., 1994). Those highly energetic charged particles penetrate though Titan's atmosphere, interacting with many molecules and leaving behind a trail of ionized and excited molecules. Ionization events generate secondary electrons with various energies (e.g., Spinks and Woods, 1964). (Electromagnetic radiation with high photon energy, such as X-rays, also produces secondary electrons by the photoelectric effect.) If the energy of these secondary electrons is less than about 100 eV, a small cluster of excited and ionized species, called a "spur," is formed. Those secondary electrons that have energy in excess of a few hundred eV form branching tracks known as δ-rays. As the energetic electrons are decelerated by collisions with molecules, the intensity of ionization and excitation increases towards the end of its path called "blobs" (Spinks and Woods, 1964). The energy consumed for the formation of an ion pair (for example, 34.7 eV for N_2 and 27.3 eV for CH_4) is about twice the ionization potential of the gas (Spinks and Woods, 1964). The excess energy is used in causing excitation, so that approximately equal amounts of energy are consumed in the ionization and excitation processes (Denaro and Jayson, 1972). About 70–80% of the total ionizations are due to secondary electrons (Denaro and Jayson, 1972). The packets of an energy of 1 MeV are broken down into packets of $\sim$ 30 eV (O'Donnell and Sangster, 1970). In the gas phase, the density of ions and excited species formed initially along the track of a charged particle and in the spurs very soon decreases as a result of diffusion and by chemical reactions. However, it is noted that the radiation chemistry with a large number of ionized and excited molecules by charged particles occurs locally along the tracks, not uniformly in Titan's atmosphere (Thompson et al., 1991).

Ions and excited molecules formed in cold plasma (in which the electron temperature is 1 to 10 eV) give rise to chemical effects similar to those produced by ionizing radiation (e.g., Spinks and Woods, 1964). In a typical ICP system, only 20–30% of the power is available as plasma in the gas because of the power loss to the coil and matching circuit (Roth, 1995). If we assume that the 25% of the power ($\sim$ 25 W) is available to plasma, the average energy dose per molecule of CH_4 and N_2 flowed through the chamber is 9–16 eV mol^{-1}, which is of the same order as the previous experiments ($\sim$ 15 eV mol^{-1} for Khare et al., 1984a, 1984b; 8.4 eV mol^{-1} for Coll et al., 1999), but slightly higher than the low-radiation-dose experiment of 1.4 eV mol^{-1} (Thomp-

son et al., 1991). Because the typical ion fraction in cold plasma is around 10^{-4}–10^{-6} (Roth, 2001), this estimation of the dose per molecule should be the upper limit.

It is difficult to estimate the energy dose per molecule and/or the local ion fractions in and around particle tracks induced by charged particle irradiations in Titan's atmosphere. Nonetheless, we believe that the ion–molecule and free radical processes in the cold plasma experiments would be relevant to the chemistry induced by the charged particle irradiation in Titan's atmosphere.

3. Results

In this section, we discuss the results of infrared spectroscopy, UV/VIS spectroscopy, two-step laser mass spectroscopy (μL^2MS), Raman spectroscopy and organic elemental analysis. Infrared spectroscopic measurements can reveal the characteristic bonding structures in tholin. UV/VIS spectroscopy may reveal the presence of multiple bonds in tholin. Analyses by μL^2MS and Raman spectroscopy are useful to reveal the presence of aromatic compounds. Finally, bulk elemental compositions of C, H, and N, are determined by organic elemental analysis. The implications of these results are discussed in Section 4.

3.1. Infrared spectroscopy

The IR transmittance of thin films of tholin deposited on KBr substrate were measured by a FT–IR spectrometer (Nicolet, Nexus 670) in the range from 7000 to 400 cm^{-1} (1.43–25.0 μm) with a resolution of 1 cm^{-1}. Blank KBr substrate was used as a reference. The FT–IR system was continuously purged with dry air. Figure 3 shows the infrared spectra of tholin formed at five different deposition pressures.

3.1.1. Characteristic frequencies in infrared spectra

All the IR spectra in Fig. 3 show the characteristics of N–H bonds (3200–3500 cm^{-1}, (3.13–2.86 μm)), C–H bonds (2800–3100 cm^{-1}, (3.57–3.23 μm)), triple bonds and cumulative double bonds such as C≡N and –N=C=N– (2000–2300 cm^{-1}, (5.00–4.35 μm)), NH_2 bending (1600 cm^{-1}, (6.25 μm)), double bonds like C=C and C=N (1500–1650 cm^{-1}, (6.67–6.06 μm)), and C–H bending (1375–1465 cm^{-1}, (7.27–6.83 μm)). The details of the possible peak assignments (Rao, 1963; Bellamy, 1975, 1980; Colthup et al., 1990; Lin-Vien et al., 1991; Socrates, 2001) are summarized in Table 2 and described in Appendix A.

The broad absorptions at 3200–3500 cm^{-1} (3.13–2.86 μm) in Fig. 3 suggest that hydrogen bondings due to N–H bonds are predominant in Titan tholins. The extension of N–H bands to frequencies lower than 2600 cm^{-1} (3.85 μm) supports the presence of strong hydrogen bonds (Lin-Vien et al., 1991, pp.164–165; Bellamy, 1980, pp. 274–281). The usual NH—N (lone-pair of saturated N atom) type hydrogen bonds or the NH—π (π electron of aromatics) type hydrogen bonds may not be strong enough to cause these broad absorptions. They may instead be caused by the strong hydrogen bondings between N–H moieties and the unsaturated N atom of the heterocyclic ring (Bellamy, 1980; Lin-Vien et al., 1991). The predominance of hydrogen bonding in tholin due to N–H bonds is very consistent with the presence of thermally stable compounds ($\sim$ 1200 K), which is indicated by the thermogravimetric analysis (Khare et al., 1981), the residue of pyrolysis GC/MS analysis (Khare et al., 1984b; Ehrenfreund et al., 1995), and the residue of organic elemental analysis (McKay, 1996).

The broad absorption features at 3500–2600 cm^{-1} (2.86–3.85 μm) are also frequently found in IR spectra of carboxylic acids because of the strong O–H hydrogen bondings (Colthup et al., 1990). These absorptions in Fig. 3, however, are not mainly due to O–H stretching vibrations, since Khare et al. (2002) also detected these broad peaks in the IR spectrum of Titan tholin, which was measured without exposure to oxygen in the air. The minor contribution of oxygen to the IR spectra is also supported by the absence of carbonyl group (C=O) absorptions around 1650–1800 cm^{-1} (6.06–5.56 μm).

3.1.2. Variation of infrared spectra due to deposition pressures

In this section, we discuss three main effects of pressure on the IR spectra.

1. Aliphatic C–H absorptions are strong in tholin formed at higher pressures but almost disappear at lower pressures in comparison with the N–H absorptions.

To compare the amount of aliphatic C–H bonds and that of N–H bonds, the integrated absorbance area of all the IR spectra were measured for C–H bands (2780–3040 cm^{-1}, (3.60–3.29 μm)) and for N–H bands (2600–3570 cm^{-1}, (3.85–2.80 μm)). The areal ratios of aliphatic C–H bands to N–H bands are given as a function of deposition pressures in Fig. 4. The areal ratio of aliphatic C–H bands to N–H bands increases monotonically with pressure. Two peaks at 1460 and 1375 cm^{-1} (6.85 and 7.27 μm) due to the $-CH_3$ bending mode also increase with pressure. There are at least four possible causes for the observed low C–H/N–H ratios at low pressures.

(1) Carbon occupies aromatic rings in tholin formed at lower pressures rather than open chain aliphatic compounds.
(2) Nitrogen is included in tholin formed at lower pressures more than carbon.
(3) Hydrogen is preferentially connected to nitrogen at low pressures more than carbon, perhaps because of the higher stability of N–H bonds (bond energy = 3.7 eV) compared to C–H bonds (bond energy = 3.5 eV).

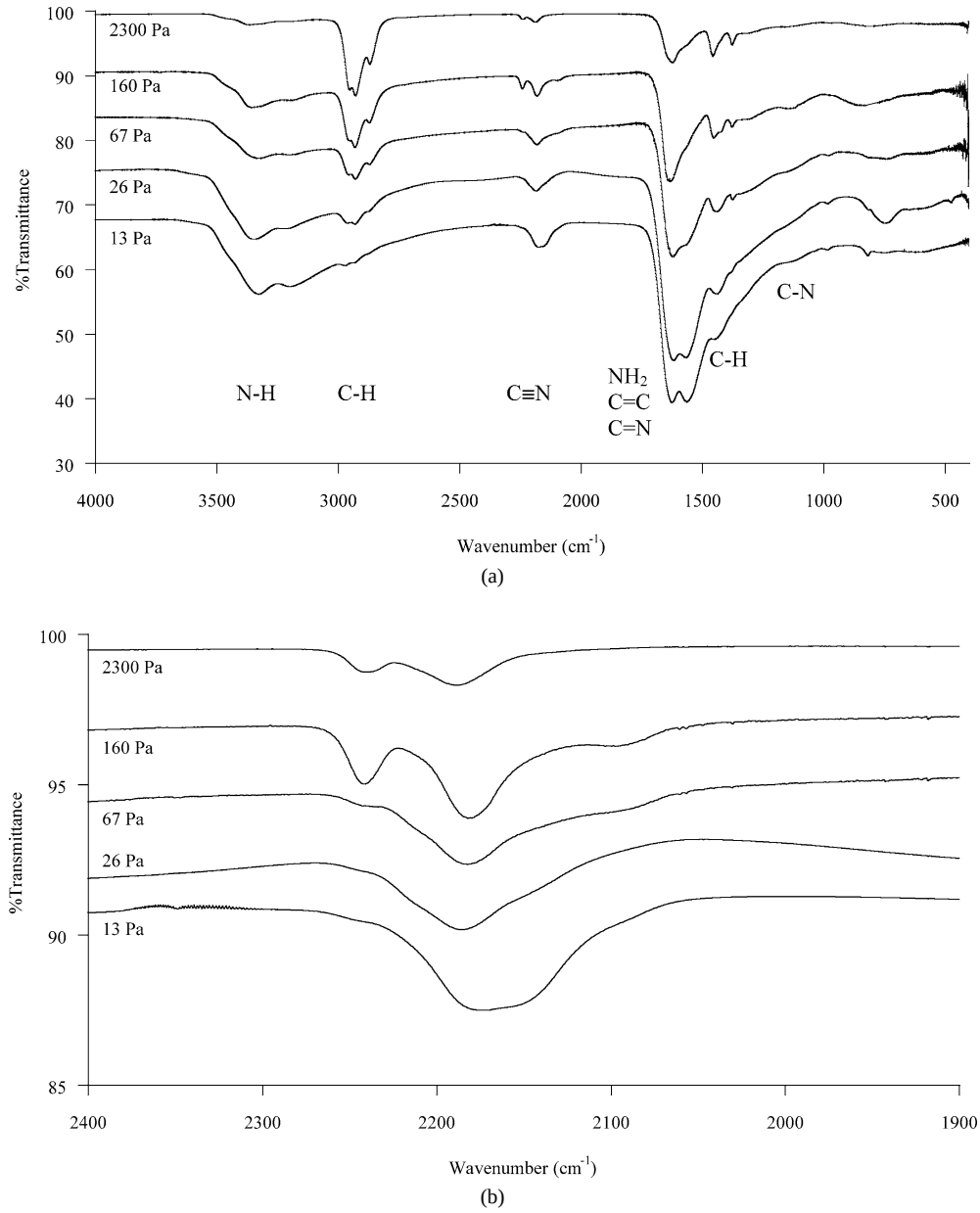

Fig. 3. Comparison of IR spectra for tholins produced by ICP discharge in CH_4/N_2 (= 10/90) gas mixture at 13, 26, 67, 160, and 2300 Pa. Intensities have been offset. (a) 4000–400 cm^{-1}, (b) extended at 2300–1900 cm^{-1}.

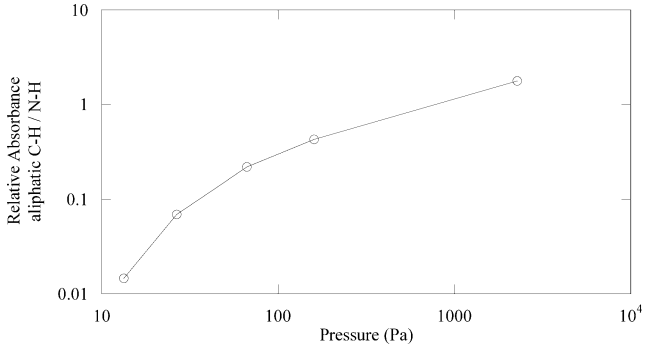

Fig. 4. Relative IR absorbance of aliphatic C–H vibration (2780 –3040 cm^{-1}) and N–H vibration (2620–3570 cm^{-1}) as a function of deposition pressures.

(4) The stronger hydrogen bond between the N–H groups and the unsaturated N atom in heterocyclic rings at lower pressures might cause the broader IR absorption of N–H bonds with an increase in intensity.

2. A doublet at 1620 and 1580 cm^{-1} (6.17 and 6.33 μm) appears in tholin formed at lower pressures.

This doublet at 1620 and 1580 cm^{-1} (6.17 and 6.33 μm) is likely to be caused by the quadrant stretch of aromatic rings (Lin-Vien et al., 1991). While the intensities of the sharp peaks at 1460 and 1375 cm^{-1} (6.85 and 7.27 μm) due to the asymmetric and symmetric $–CH_3$ bending modes decrease, a broad peak at 1450 cm^{-1} (6.90 μm) due to the

Table 2
Characteristic frequency of IR absorption spectra obtained from tholins formed at various pressures

Frequency (ν) cm^{-1}	Wavelength (λ) μm	Implied functional group	Intensity[a]				
			13 Pa	26 Pa	67 Pa	160 Pa	2300 Pa
3450	2.90	–NH– stretching (aromatic)	w, sh	w, sh	w, sh	w, sh	w, sh
3324–3366	2.97–3.01	$–NH_2$ asymmetric stretching, –NH– stretching	s	s	m	m	w
3320	3.01	$–NH_2$ symmetric stretching				w, sh	w, sh
3190–3215	3.11–3.13	–NH– stretching or overtone of $–NH_2$ bending	s	s	m	m	w
2954–2972	3.36–3.39	$–CH_3$ asymmetric stretching	w	m	s	s	vs
2929–2932	3.41	$–CH_2–$ asymmetric stretching	w	m	s	s	vs
2869–2874	3.48–3.49	$–CH_3$ symmetric stretching	w, sh	m	s	s	vs
2730	3.66	–N–CH_3 or –N–$CH_2–$ (?)				vw	w
2240	4.46	R–C≡N stretching				m	w
2173–2189	4.37–4.60	Conjugated –C≡N, such as with –C=C($–NH_2$) C–N≡C stretching	m	m	m	m	m
2093–2152	4.65–4.78	–N=C=N–	m	w, sh	sh	m	
1617–1636	6.11–6.18	$R–NH_2$ scissors bending C=C stretching conjugated with –C≡N N–C=N– $N_2C=N–$ $C_2C=N–$ >C=N–N=C< Aromatics (quadrant stretch)	vs	vs	s	s	m
1565–1579	6.33–6.39	Aromatics (quadrant stretch)	vs	vs	m	sh	w, sh
1460	6.85	C–CH_3 asymmetric bending				s	vs
1440–1450	6.90–6.94	Aromatics (semicircle stretch)	w, b	m, b	s, b		
1424	7.02	$=CH_2$ scissors bending				m	w
1375–1379	7.25–7.27	C–CH_3 umbrella symmetric bending	w, sh	w, sh	m	m	s
1312–1346	7.43–7.62	C–N stretching (aromatic)	w, sh	w, sh	w	sh, b	w
1142–1158	8.64–8.76	C–N stretching (aliphatic)	w, b		sh	w	w
977–986	10.1–10.2	Vinyl C–H bending	m	m	m	w	w
800–900	11.1–12.5	C–N stretching (aliphatic)				m,b	m,b
818	12.2	C–H wag (aromatics)	m	sh	sh		
740–760	13.2–13.5	Aromatics	w, b	m	m		
560–650	15.4–17.9	Aromatics	w, b	w	w, b	w,b	
475	21.1	Aromatics		w			

[a] Very strong (vs), strong (s), medium (m), weak (w), broad (b), shoulder (sh).

semicircle stretching of aromatics (Lin-Vien et al., 1991) increases at lower pressures. Nitrogen containing heteroaromatics also have these ring stretching vibration bands between 1625–1430 cm^{-1} (6.15–6.99 μm) (Socrates, 2001). In addition to the appearance of ring stretching bands, the peaks due to the out-of-phase C–H wag modes of aromatics at 818 and 750 cm^{-1} (12.2 and 13.3 μm) are observed at low pressures. All these peaks that appeared at lower pressures are consistent with the presence of aromatic rings including nitrogen heteroaromatic rings. It is worthwhile noting that the 1580 cm^{-1} (6.33 μm) band is intensified considerably in the case of conjugation with fused ring systems (Bellamy, 1975; Socrates, 2001). The appearance of a 1580 cm^{-1} (6.33 μm) band suggests the presence of fused ring systems in tholin formed at low pressures. The peaks at 1580, 1450, 818, and 750 cm^{-1} (6.33, 6.70, 12.2, and 13.3 μm) observed in tholin formed at low pressures also agree with the IR characteristics of some N-PACs, which have recently been measured by matrix isolation techniques (Mattioda et al., 2003).

3. The bands around 2000–2300 cm^{-1} (5.00–4.35 μm) vary greatly with deposition pressure (Fig. 3(b)).

Cumulative double bonds and triple bonds, such as –N=C=N– and C≡N, have characteristic frequencies in this region. Because tholins are large complex heteropolymers, they are unlikely to have a large abundance of asymmetric C≡C bonds, which is needed to be IR-active (Lin-Vien et al., 1991). Here, we focus on nitrogen related functional groups. It is well known that the intensity and frequency of C≡N stretching bands depend considerably on their environmental factors (Rao, 1963; Bellamy, 1980; Lin-Vien et al., 1991; Bernstein et al., 1997). Those bands at 2000–2300 cm^{-1} (5.00–4.35 μm) were decomposed into seven Gaussians (Fig. 5(a)). These peaks are assigned to be aliphatic nitriles (2240 cm^{-1}, (4.46 μm)) aromatic nitriles (2210, 2230 cm^{-1}, (4.52, 4.48 μm)), conjugated nitriles such as $(NH_2)>C=C<C\equiv N$ (2180 cm^{-1}, (4.59 μm)), carbon diimide or aliphatic isocyanide (2150 cm^{-1}, (4.65 μm)), aryl isocyanide (2135 cm^{-1}, (4.68 μm)), and ketene imines

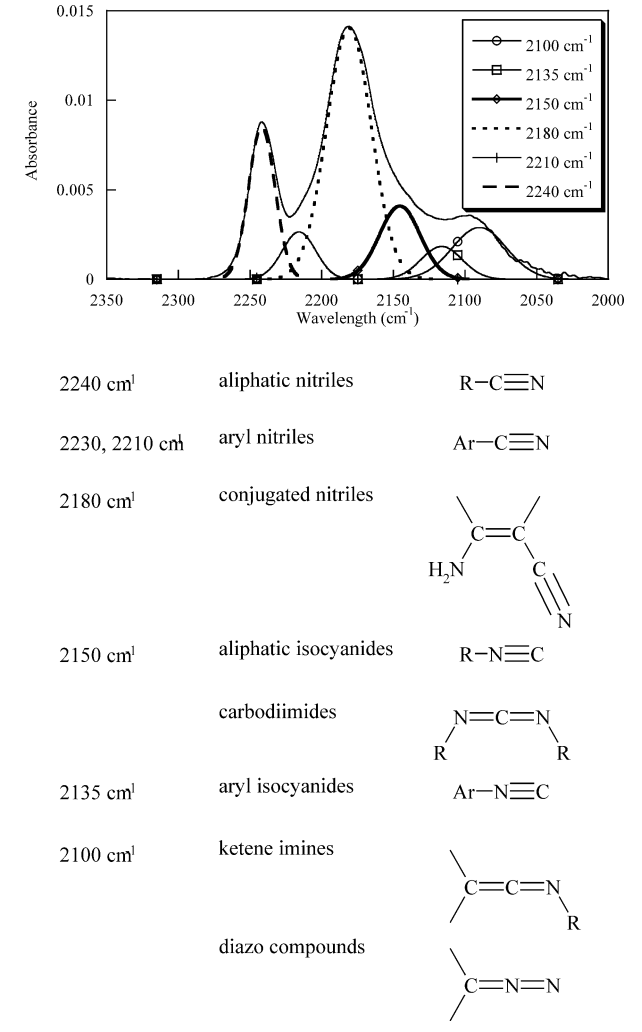

Fig. 5. (a) The 2350–2000 cm^{-1} region of IR spectra for 160 Pa tholin fit with a decomposition of seven Gaussians modeling nitrogen-containing groups. (b) Change in relative strengths of Gaussians normalized to total areal intensity of seven Gaussians as a function of deposition pressures.

or diazo compounds (2100 cm^{-1}, (4.76 μm)). The area of each Gaussian was measured and normalized with the total absorbance from 2000–2300 cm^{-1} (5.00–4.35 μm). The relative absorbances of all the bands change with pressure (Fig. 5(b)), which suggests that the way nitrogen is incorporated into structure changes substantially with pressure. At higher deposition pressures, nitriles are bonded as a terminal group, such as aliphatic nitriles (R–C≡N) and conjugated nitriles ($(NH_2)>C=C<(C\equiv N)$, etc.). At lower pressures, nitrogen is more likely to be included in carbon networks, such as carbon diimides (–N=C=N–) or isocyanides (C–N≡C).

In summary, we observed a decrease in aliphatic C–H bonds and an increase in aromatic ring stretching in tholin formed at lower pressures. Nitrogen tends to be incorporated into the carbon networks at lower pressures. These IR spectra analyses suggest the presence of nitrogen-containing heteroaromatics in tholin formed at lower pressures.

3.2. UV/VIS spectroscopy

It has long been known that colored substances, chromophores, owe their color to the presence of one or more unsaturated linkages (e.g., Rao, 1975). Saturated organic molecules exhibit little absorption in the near ultra-violet and visible regions (200–800 nm). The absorption tails in visible wavelengths indicate the presence of delocalized π electrons, which are due to fused aromatic rings and conjugated multiple bonds. The wavelength corresponding to the absorption maximum depends on environmental factors, such as the electronegativities of the elements forming the double bond. The color shift and strength variation are also caused by the auxochromes which contains lone-pair electrons, such as –OH, –OR, –NHR, and $–NR_2$ (Rao, 1975).

Transmittance and reflectance by thin films of tholin deposited on CaF_2 and quartz substrates were measured with a UV/VIS/NIR spectrometer (Perkin Elmer, Lambda 900) in the range of 185 to 3300 nm. The film thickness was measured with a profiler (Sloan Tech. Corp., Dektalk 2A). The k-value, the imaginary part of the optical constants, was obtained from

$$k = \frac{\lambda}{4\pi d} \ln\left[\frac{T_s(1-R)}{T(1-R_s)^2}\right].$$

Here, λ is wavelength, d is thickness, T and R are measured transmittance and reflectance for the thin film, and T_s and R_s are those for the substrate. The method is described by Khare et al. (1984a).

Figure 6 shows the calculated k-values. The k-value increases when the pressure is lowered from 2300 to 26 Pa, and remains the same between 26 and 13 Pa. This shift in the slope of k-value corresponds to the change in color from the yellowish films at higher pressure to the dark brownish films at lower pressures. The differences in k-values at pressures between 26–2300 Pa are larger than the error of 20% that is attributed to uncertainty in the determination of thickness. The absorption tails at visible wavelengths indicate that the delocalized π electrons exist in significant amounts, especially in tholin formed at lower pressures. Figure 7(a) shows the dependence of the k-value on the deposition pressure at some selected wavelengths, such as 0.42, 0.50, 0.58, and

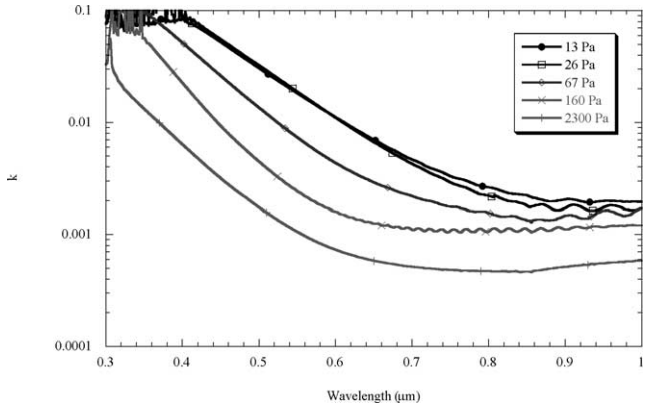

Fig. 6. Imaginary part of the optical constants (k value) for Titan tholins formed at various pressures, in UV/VIS region.

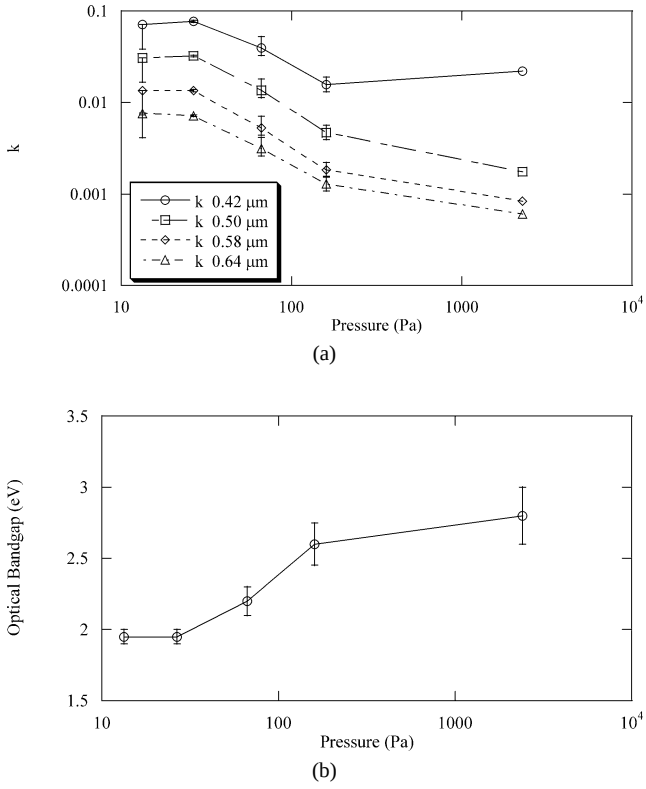

Fig. 7. (a) Variation of the k-values at selected wavelengths as a function of deposition pressures. Error bars are from thickness measurements. (b) Variation of the optical band gap (Tauc gap) as a function of deposition pressures.

0.64 μm (corresponding to the filters of the Voyager imaging camera). The error bars from the thickness measurements are also shown in Fig. 7(a). While the k-value at 0.42 μm does not change very much with pressure, the k-value of tholin formed at lower pressure is considerably larger at the longer wavelengths. This stronger absorption in visible light suggests the presence of increased abundance of fused aromatics of larger cluster size at lower pressures. The stronger absorbance could also be caused by longer conjugated polyenes formed at lower pressure, if the conjugated polyenes would be a dominant structure in tholin. However, as discussed later, the very long conjugated polyenes would not be a dominant structure in tholin under the charged particle irradiation, because they are less stable than aromatics.

The optical band gap E_g is expected to decrease with the number of rings per cluster (Robertson and O'Reilly, 1987). E_g was determined from the absorption coefficient α ($= 4\pi k/\lambda$) as the intercept found from plotting $\sqrt{\alpha E} = B(E - E_g)$ (Tauc, 1972). The decrease in the optical band gap for decreasing deposition pressure (Fig. 7(b)) again suggests the larger size of fused aromatics rings in tholin formed at lower pressures.

3.3. Two step laser mass spectroscopy

Thin films of tholin deposited on aluminum were investigated by microprobe laser-desorption, laser-ionization mass spectrometry (μL^{2}MS), a sensitive and selective technique for detecting aromatic compounds. Neutral molecules were desorbed from the tholin using an IR laser, ionized by a UV laser at 266 nm, and then detected with a reflectron time-of-flight mass spectrometer. A detailed explanation of the method is given by Clemett and Zare (1997). The μL^{2}MS method is able to detect PAHs and complex aromatics, including nitrogen-containing heteroaromatics. However it has much less sensitivity to olefins under the conditions used in this study. In this study, three 50-shot averages were taken of each aluminum-deposited tholin. Deuterated toluene was used as a calibrant and was leaked at a steady rate into the μL^{2}MS instrument.

The μL^{2}MS spectra of the tholins show the presence of a complex organic mixture containing a variety of aromatics up to 300 amu in mass and suggest a predominant amount of one- to two-ring compounds with extensive side-chain addition (see Fig. 8(a)). Exact identification of mass peaks is difficult because of the complexity of the mass spectra. Alkylation was indicated by the presence of a 14-amu spacing pattern caused by addition of –CH_2– groups to parent aromatics. Addition of –NH– groups was also indicated by the presence of peaks with 15 amu spacing. The cluster of peaks spaced at 1 amu apart suggests the extensive substitutions of nitrogen into the aromatic compounds. Simple PAHs such as naphthalene (128 amu) and phenanthrene (178 amu) were not observed. The shape of the mass spectra remained similar for different plasma pressure conditions, although the intensities of the mass peaks increased when the pressure was decreased.

The μL^{2}MS method is a semi-quantitative technique, in which the same intensities of two peaks do not necessarily indicate the same concentration of the two species. A change in the relative intensities of the same peak, however, can be used as a quantitative scale. To compare relative amounts of aromatics in tholins deposited under different pressures, the integrated area of the 105–300 amu region was compared to the area of the calibrant d_8-toluene peaks (100 amu) in each mass spectrum. The resulting aromatic/toluene ratios

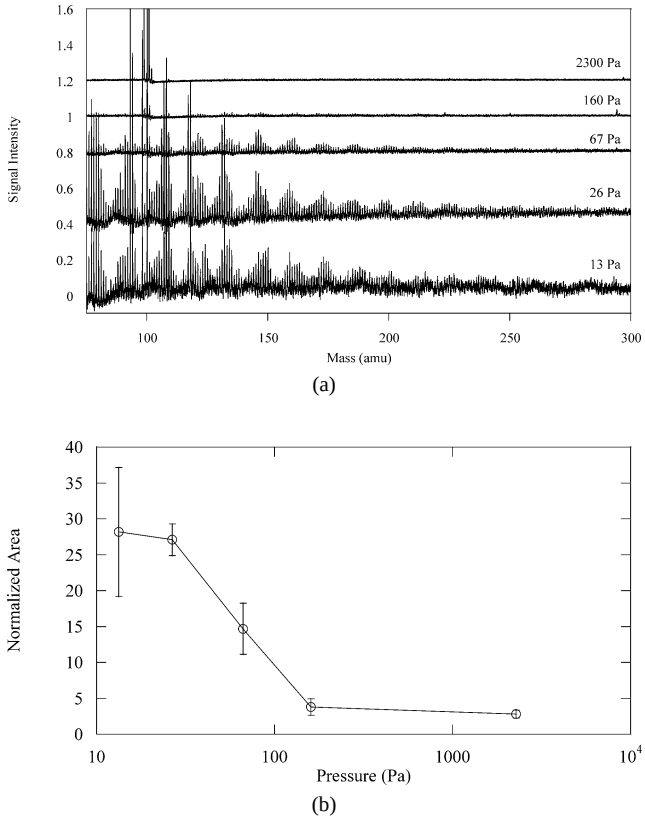

Fig. 8. (a) Mass spectra of Titan tholins formed at various pressures, obtained by μL^2MS. Each of the intensities was normalized to the intensity of deuterated toluene (100 amu), which was introduced for calibration. Intensities have been offset. (b) Variation of the integrated peak area of μL^2MS spectra (between 100–300 amu) as a function of deposition pressures. Areas were normalized to the area of the deuterated toluene (peak at 100 amu) used as a calibrant.

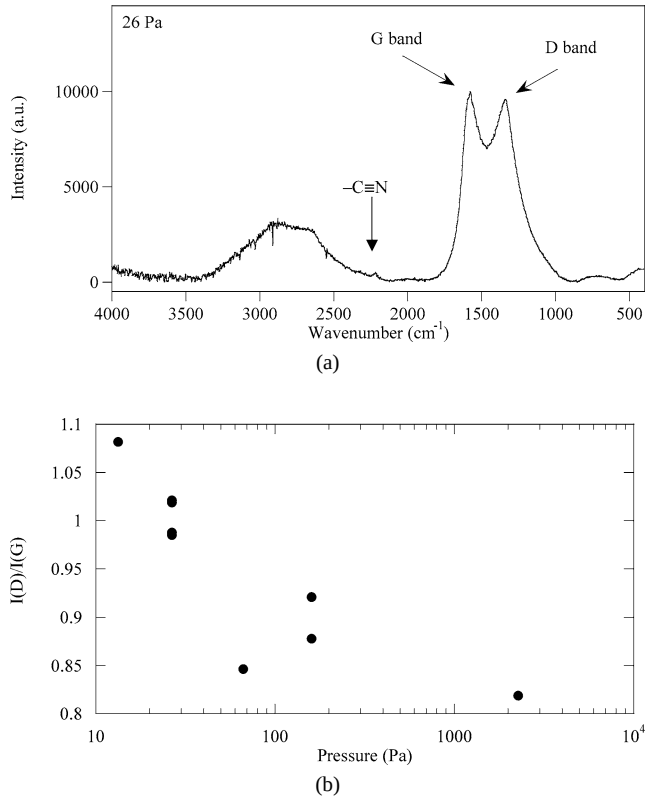

Fig. 9. (a) Typical Raman spectrum of Titan tholin formed at 26 Pa. The G-band and D-band are clearly seen. (b) The intensity ratio of the D-band and G-band, $I(D)/(G)$, as a function of deposition pressures.

for each pressure are shown in Fig. 8(b). At lower pressures, the aromatic/toluene ratio was greater than at higher pressures, suggesting the increase of aromatic formation at lower pressures. At 2300 Pa, the highest pressure studied, no aromatics were detected by μL^2MS.

Our results differ markedly from those seen by Sagan et al. (1993), who observed no nitrogen incorporations (no odd mass peaks) in their mass spectra. They found instead clear peaks corresponding to the alkylated series of phenanthrene (178, 192, 206, 220 amu) as well as other unalkylated PAHs (for example, pyrene at 202 amu). The cause of these differences is not yet understood, but is possibly due to differences in experimental conditions or measurement conditions.

3.4. Raman analyses

Raman spectroscopy is a widely used technique to characterize amorphous carbon species (e.g., Tamor and Vassell, 1994). In amorphous carbon, the G band at 1500–1600 cm^{-1} (6.67–6.25 μm) arises from the bond stretching motion of pairs of sp^2 C atoms, in aromatic rings or olefinic chains. The D band at $\sim$ 1350 cm^{-1} (7.4 μm) arises from the breathing modes of sp^2 atoms in clusters of six-fold aromatic rings. There is no D mode if the sp^2 sites form only olefinic chains. For amorphous carbon, the disorder is so great that the intensity ratio of the D and G modes, $I(D)/I(G)$, decreases with decreasing cluster size of fused aromatic rings (Ferrari and Robertson, 2000; Rodil et al., 2001).

The Raman spectra were recorded in the 100–4200 cm^{-1} region in the back-scattering mode with a Nicolet Almega 670 spectrometer (excitation 532 nm Ar laser). A typical Raman spectrum of tholin formed at 26 Pa after the subtraction of the broad signal due to fluorescence is shown in Fig. 9(a). The peaks of G-band and D-band are clearly seen. These two peaks were decomposed into Gaussians and the intensities were measured. The intensity ratio of D bands to G bands, $I(D)/I(G)$, increases when the deposition pressure decreases (Fig. 9(b)). If we neglect the effect of nitrogen on the $I(D)/I(G)$ ratio, this increase suggests a larger cluster size of aromatic rings at lower pressure (Ferrari and Robertson, 2000; Rodil et al., 2001). Evidence of nitriles (C≡N) is also seen in the Raman spectrum. Because the fluorescence is very strong in our sample, it was necessary to use high laser power to obtain high enough signal-to-noise ratio. Most of the samples were annealed by the laser beam used for analysis, and some structures could be changed by the annealing. Nevertheless, the variation of the $I(D)/I(G)$ ratios suggest the structure variation of aromatics in tholins.

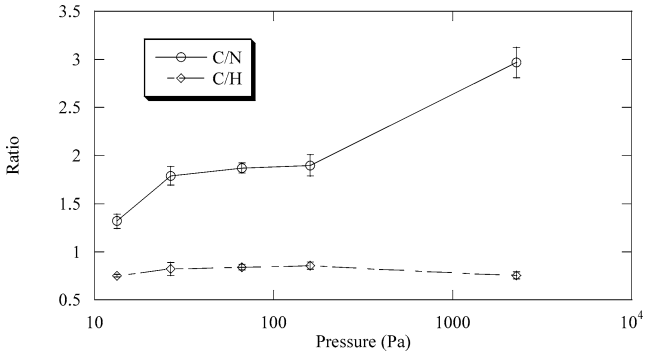

Fig. 10. Variation of elemental compositions (C/N and C/H) in tholin as a function of deposition pressures. Tholins were formed more than twice with the same experimental conditions. At least four samples from each experimental run were measured by two independent instruments for elemental analysis.

3.5. Elemental analysis

The C/H/N compositions of tholin collected by scratching the deposited films were determined by conventional organic elemental analysis (i.e., combustion method). Figure 10 shows a variation of C/N and C/H as a function of deposition pressure. Error bars were determined by conducting experiments more than twice with the same conditions. At least four samples from each experimental run are measured by two independent instruments (Thermo Quest 1100 NA at NASA Ames Research Center, and Perkin Elmer PE240 at Galbraith Lab. Inc., TN). The decrease in C/N for decreasing pressure shows that nitrogen is more abundant in tholin formed at lower pressures. Between 26 and 160 Pa, however, the C/N and C/H ratios do not change significantly. In this pressure range (26–160 Pa), we have observed significant changes in infrared spectra, k-values, and in the intensity of μL^2MS peaks. The lack of change in elemental ratios implies that the cause of these other changes is structural, rather than compositional, with possible causes such as a conversion from open-chain olefins to heteroaromatic ring structures (Fig. 11(b)). It is worthwhile noticing that this conversion from even a conjugated olefinic system to an aromatic system dramatically increases the stability of the molecule due to the achievement of the $(4n + 2)$ π electron in the delocalized ring system (Hückel's rule). IR spectra show the decrease of aliphatic C–H bonds ($–CH_3$) and the increase of N–H bonds ($–NH_2$) when the pressure decreases in this range (Section 3.1.2). The substitution of $–CH_3$ with $–NH_2$ may lead to the excess hydrogen in tholin. It is noticed that the triple bonds of aliphatic nitriles (–CN) decrease when the pressure decreases. One of the possible structural changes is that the net excess hydrogen would add to the triple bond of nitriles (–CN) forming structures such as (>C=N–H). The increase of IR absorption at ~ 1620 cm^{-1} (C=N bonds) (Fig. 3) is also consistent with this view.

4. Discussion

In this section, we first summarize the results discussed in Section 3 and discuss the implications of the pressure effects on tholin structures and formation processes. Then, we investigate how plasma properties depend on deposition pressure and discuss experimental parameters other than pressure in Section 4.2. Comparisons with previous tholin studies are discussed in Section 4.3. Finally, we discuss the implications for the structures of Titan's haze and their role in Titan's atmospheric thermal structure and complex organic chemistry.

4.1. Tholin structure and its formation

Our experimental results are summarized in Table 3. IR spectroscopy suggests that the amounts of both aromatic and heteroaromatic rings are higher in tholin formed at lower pressures. The decrease in saturated aliphatic C–H stretching bands is consistent with the increase in unsaturated aromatic rings, although aromatic C–H stretching bands are not clearly observed. The presence of aromatic rings, possibly fused ring systems, is suggested. In tholin formed at higher pressures, nitrogen is likely to be found in a terminal group such as $–NH_2$ or –C≡N. However, nitrogen is incorporated into carbon networks, such as –NH–, –N=C=N–, or –N≡C at lower pressures.

The analyses by UV/VIS absorption spectroscopy show that tholin formed at lower pressures contains more delocalized π electrons, suggesting the presence of larger amounts of fused aromatic rings with larger cluster size, which are confirmed with μL^2MS and Raman spectroscopy. The abundant incorporation of nitrogen into tholin formed at low pressures is suggested with the decrease in C/N ratio at lower deposition pressures. Thus, the presence of the nitrogen-containing polycyclic aromatic compounds (N-PACs) in tholin formed at low pressures is strongly suggested. Their delocalized π electrons may dominate the optical properties of tholin.

However, the aromatic components are likely to be present only in trace amounts in tholin. Previous results of μL^2MS showed that PAHs are present on the order of 10^{-4} g g^{-1} of Titan tholin (Sagan et al., 1993). NMR analysis suggests the aromatic compounds would be at most 25% (Sagan et al., 1993). Although the aromatics are only minor compounds, they play a dominant role in absorbing the UV/VIS light.

These analyses give us a general picture of the tholin structures. Tholin formed at low pressures contains the clusters of nitrogen-containing polycyclic aromatic compounds (N-PACs) in a matrix of carbon and nitrogen chain/branch networks, such as $(–NH–CH_2–)_n$ and $(–(NH_2)C=C(–C≡N)–)_n$, which are connected tightly to each other with hydrogen bonding. At higher deposition pressures (2300 Pa), the polymer-like chain structure terminated with $–CH_3$ and –C≡N may be formed with fewer aromatic compounds.

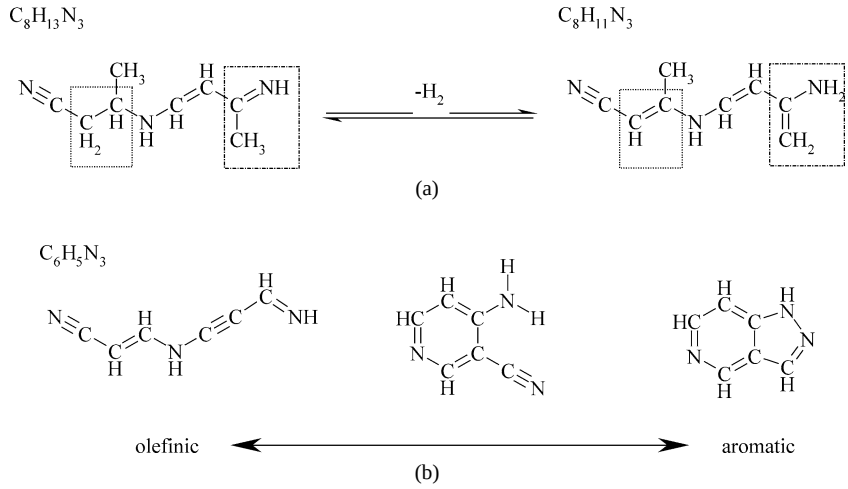

Fig. 11. Possible explanations for the structure differences of the tholins at different pressures. (a) Attachment of hydrogen to the unsaturated bonds making saturated C–H bonds (in dotted line) and movement of hydrogen from C–H bonds to more stable N–H bonds (in dashed line). (b) Conversion from olefinic structures to aromatic structures without changing elemental ratios.

Table 3
Summary of tholins formed at various pressures in cold plasma

Cold plasma	Deposition pressure (altitude in Titan)	13 Pa (280 km)	26 Pa (250 km)	67 Pa (210 km)	160 Pa (170 km)	2300 Pa (75 km)
IR spectroscopy[a]	Aliphatic hydrocarbons	–	w	m	s	vs
	Amines	vs	vs	s	s	w
	Conjugated C=C with C=N	s	s	s	s	s
	Aromatic rings	s	s	m	w	–
	Nitrogen position	C=N=C, –NC	C=N=C, –NC	C=N=C, –NC	–CN	–CN
UV/VIS spectroscopy	Color & morphology	Brown film	Brown film	Brown film & yellow powder	Yellow film & yellow powder	Yellow/red film
	k value at 0.5 μm	0.031	0.032	0.014	0.0047	0.0018
	optical gap (Eg)	1.9 eV	1.9 eV	2.2 eV	2.6 eV	2.8 eV
μL^2MS[a]	Intensity: amount of aromatics	vs	vs	s	m	–
Raman spectroscopy	$I(D)/I(G)$: size of ring	large	large	medium	medium	small
Elemental analysis	C/N	1.45	1.78	1.85	1.97	2.76
	C/H	0.75	0.8	0.8	0.79	0.73
Optical emission spectroscopy (UV/VIS)	UV intensity (300–400 nm)	low	middle	middle	middle	high
	N_2^+/N_2	middle	middle	high	high	very low
Gas analysis by GC/MS (Thompson et al., 1991)	Pressure in cold plasma		24 Pa			1700 Pa
	Gas species		unsaturated			saturated
	G_{tot}, product $(C+N)/100$ eV		0.79			4.0

[a] Intensity: very strong (vs), strong (s), medium (m), weak (w).

Thompson et al. (1991) found an increase in the amount of unsaturated hydrocarbons in gas-phase products formed at lower pressures (Table 3). The experimental results of our study suggest that the amount of aromatic and heteroaromatic rings may be greater in tholin formed at lower pressures. These results suggest that fewer collisions of multiple bonds with hydrogen at lower pressure maintain unsaturated compounds in gas phase products and lead to unsaturated ring structures in the solid products (Fig. 11(a)). Hydrogen may prevent those aromatic rings and conjugated olefins from growing larger and longer by the termination with $–CH_3$ and $–NH_2$. Alternatively, collisions with higher energy electrons and ions/radicals at the surface of the tholin in lower deposition pressures may break aliphatic C–H bonds, removing hydrogen from the tholin surface and forming the stable aromatic rings in tholin (Fig. 11(a)). The structural conversions from open-chain olefins to aromatic ring structures (Fig. 11(b)) may also occur due to the greater stability of aromatics (Hückel's rule). The higher electron temperature in a low pressure plasma could dissociate stable N_2 bonds more effectively, allowing the formation of HCN and NH_3. This may lead to incorporation of nitrogen into the tholin. Once nitrogen is incorporated into the tholin, the stable hydrogen bonds are formed with their polar C–N bonds and N–H bonds.

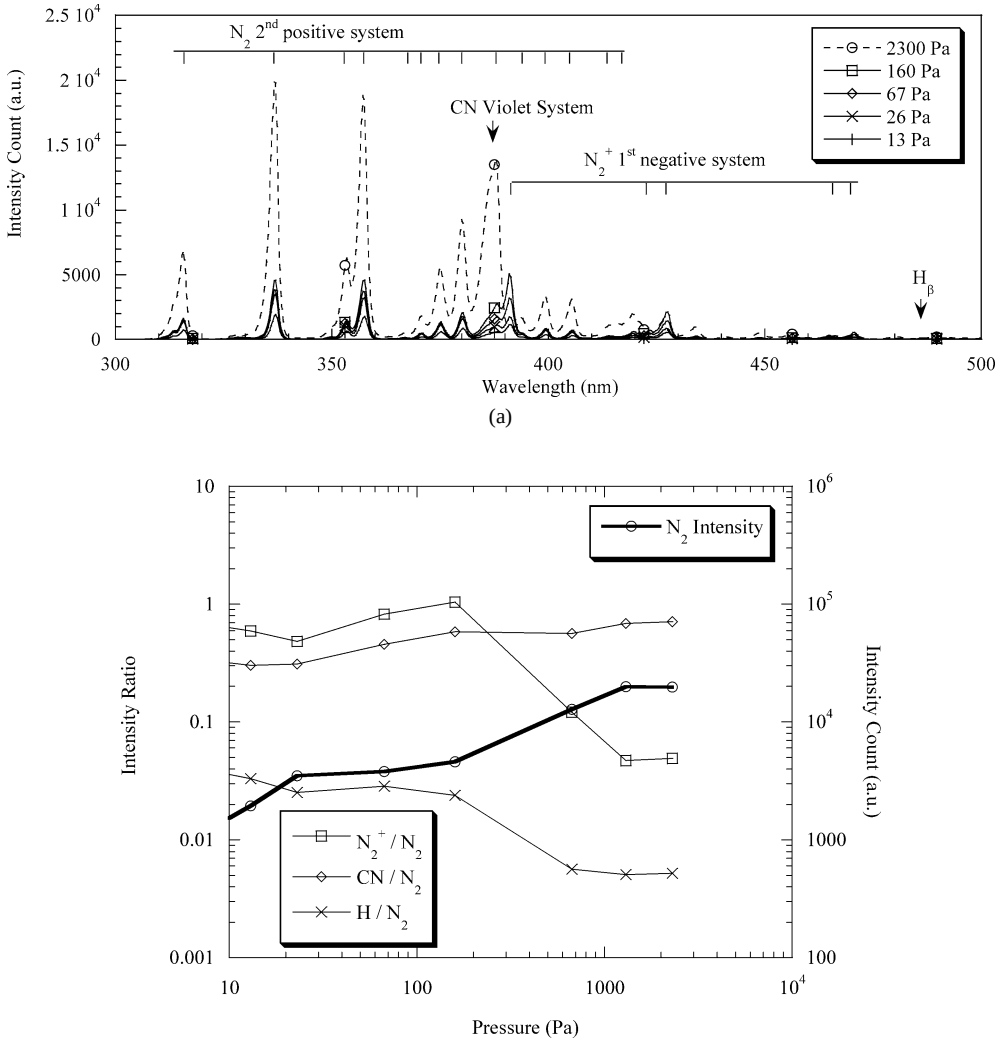

Fig. 12. (a) UV/VIS emission spectra from cold plasma ($CH_4/N_2 = 10/90$, 100 W) regions measured at various pressures. N_2 (2nd positive system, $C^3\Pi_u$–$B^3\Pi_g$), N_2^+ (1st negative system, $B^2\Sigma_u^+$–$X^2\Sigma_g^+$), CN (violet system, $B^2\Sigma$–$X^2\Sigma$), and H atom (Balmer β) are identified. (b) Intensity of the N_2 peak (337 nm) as a function of pressures. Relative intensities of the N_2^+ (391 nm), CN (388 nm), and H (486 nm) to the N_2 (337 nm) are shown as a function of pressures.

4.2. Experimental parameters other than deposition pressure

In the previous section, we have discussed the pressure dependence of chemical and optical properties of tholin. Here, we investigate how plasma properties depend on pressure. Then we discuss other possible factors that may control the properties of tholins.

4.2.1. Pressure effect on plasma states

We have shown that the chemical and optical properties depend on the deposition pressure. However, the variation in deposition pressure may change not only the collision frequencies of molecules/atoms but also the plasma properties and dose rate, such as the intensity of UV emission, the charged particles flux, and the electron temperature.

To investigate the plasma properties, the UV/VIS emission was measured with a CCD-array spectrometer (Ocean Optics, S2000) with an optical fiber though the Pyrex glass window of the chamber. Figure 12 shows results of UV/VIS emission spectra taken from plasma region at various pressures. The measurement conditions, such as the integration time of the spectrometer and the position of the optical fiber, were fixed for every measurement. Several excited chemical species of N_2 (2nd positive system, $C^3\Pi_u$–$B^3\Pi_g$), N_2^+ (1st negative system, $B^2\Sigma_u^+$–$X^2\Sigma_g^+$), CN (violet system, $B^2\Sigma$–$X^2\Sigma$), and H atom (Balmer β) are identified (Fig. 12(a)) (Pearse and Gaydon, 1976). Although the intensities are not calibrated, the relative intensity is still valid for discussions below. The intensity of UV emission by N_2 (300–400 nm) increased when pressure increased (Fig. 12(b)). The relative ratios of excited chemical species also depended considerably on pressures. Figure 12(b) shows more quantitatively

the ratios of intensities of N_2^+ (391 nm), CN (388 nm), and H (486 nm) to that of the N_2 (337 nm) as functions of pressure. At low pressures, the presence of N_2^+ ions and H atoms are indicated. The intensity due to N_2^+ ion emission is very small at 2300 Pa, while the CN radical bands are clearly seen only at 2300 Pa.

The presence of the N_2^+ ion in the lower pressure plasma suggests that the ion–molecule reactions in the gas phase are likely to play a dominant role in tholin forming processes at lower pressures. The variations of excited species at different pressures, such as N_2^+ ions at lower pressures and CN radicals at higher pressures, may change the subsequent chemical reactions in the gas phase significantly. The plasma state of a DC arc is known to shift from a disequilibrium cold plasma to a local thermal equilibrium hot plasma in the range of 10^3–10^4 Pa (e.g., Roth, 1995), implying that completely different chemical reactions may be responsible for the variation of excited species at different pressures in this study.

The electrons and charged particles collide with the surface of tholin. This may cause a change in the structure of the tholin surface, such as cross-linking or degradation (Wilson, 1974, Chapter 7). During cross-linking, cleavage of a C–H bond on a polymer chain to form a hydrogen atom is followed by abstraction of a second hydrogen atom from a neighboring chain to produce a hydrogen molecule (O'Donnell and Sangster, 1970). If hydrogen abstraction occurred at the site of adjacent C–H bonds, unsaturated bonds would be formed in tholin. This may help the formation of the aromatics or olefins. The appearance of atomic hydrogen in emission spectra at lower pressures might be consistent with this view. During radiation, aromatics would selectively survive, since polymers containing aromatics rings are known to be resistant to radiation (O'Donnell and Sangster, 1970).

Furthermore, the variation of the intensity and wavelength of the emitted UV light is likely to affect the relative importance of photochemistry and radiation chemistry in the gas phase. The larger intensity of UV light observed in plasma regions at higher pressures (due to the N_2, 2nd positive system, around 300–400 nm) suggests that photochemistry may play a more important role at higher pressures in these experiments. The coincidence of the pressure effect between UV intensity (Fig. 12(b)) and C/N ratio in tholin (Fig. 10) implies that the increase of C/N ratio of tholin might be caused by the photochemical reactions responsible for incorporating carbon into tholin. However, the quantitative ratio of the photochemistry and radiation chemistry is not well estimated, since the wavelength region below 300 nm was not observed in this study.

4.2.2. Inhomogeneous reactions

It was observed that both yellowish powders and brownish films formed at deposition pressures of 67 and 160 Pa in some very localized areas on the chamber wall (Table 3). At the lower pressures of 26 and 13 Pa and the higher pressure of 2300 Pa, those yellowish powders were not observed. The elemental ratios of these yellowish powders were determined to be C/N = 3 and C/H = 0.6 (Fig. 15). These elemental ratios were very close to that of the tholin film formed at 2300 Pa, which was a yellowish transparent film. This suggests that several tholin forming chemical reactions may occur and that the main chemical reaction may change from one mode to another around 100 Pa. This change may be the transition from two-body reactions to three-body reactions, and/or the shifts of relative importance of C_2H_2/HCN gases, and/or the relative importance of the photochemistry to the radiation chemistry. However, all the spectroscopic results described in this paper are based on the measurements of the films without yellowish powders. The slightly yellowish tholin film formed at 160 Pa and dark brownish tholin film formed at 67 and 23 Pa have almost the same C/N ratio but a different ratio of aromatic/aliphatic compounds.

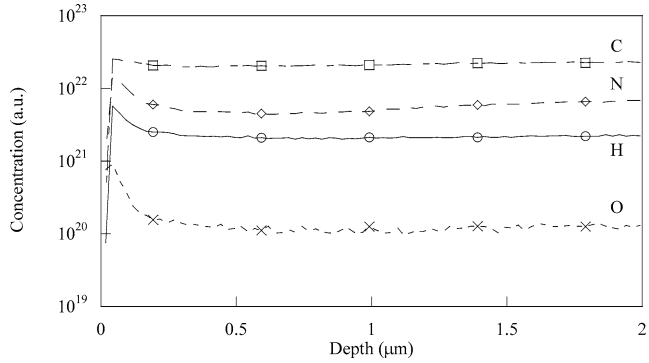

Fig. 13. Depth profile of chemical composition of tholin formed at 26 Pa determined by secondary ion mass spectrometer (SIMS).

4.2.3. Total deposition time dependence

To examine the dependence on total deposition time, we compared the IR absorbance spectra of tholin made at 26 Pa for 1, 3, 5, and 9 hr of deposition times. The absorbance of each peak is approximately in proportion to the duration of deposition, indicating that the chemical properties of tholin depend little on the total deposition time. In order to check the depth profile of chemical composition of tholin, the 3.4 μm thick film deposited on silicon at 26 Pa for 5 hr was analyzed with a secondary ion mass spectrometer (SIMS) using 10 keV Cs^+ ions (Cameca IMS-3f). The elemental composition does not show a significant variation with depth (Fig. 13), also supporting the contention that the chemical composition does not depend on the deposition time. The slight increase in each element including oxygen within 0.2 μm from the surface may be either due to the instability of the measurements in the beginning or due to surface oxidization. Since SIMS analysis was done three months after the tholin formation, the oxidization at the surface of the tholin film affects at most 0.2 μm depth (total thickness, 3.4 μm) in three months.

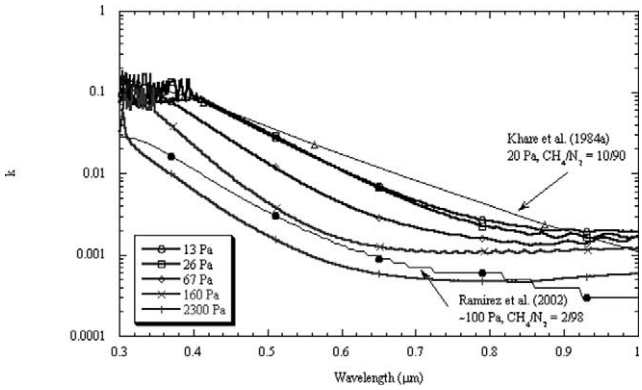

Fig. 14. Comparison of the k values of tholins formed at different pressures with the previous laboratory works (Khare et al., 1984a; Ramirez et al., 2002).

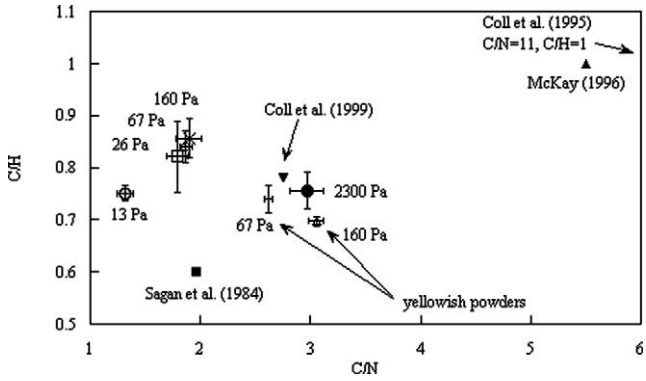

Fig. 15. Comparison of elemental ratios (C/N and C/H) with previous laboratory work. All tholins were created by electrical discharge in methane/nitrogen gas mixtures.

4.3. Comparison with previous tholin studies

We compare the spectral properties and chemical compositions of our tholins with the previous tholin studies, focusing on the effect of experimental conditions, such as the pressure, temperature, and initial gas compositions. Table 4 presents the summary of previous studies on tholin formed by an electrical discharge.

The IR spectrum of tholin formed at 20 Pa by Khare et al. (1984a) resembles our tholin formed at lower pressures (13–26 Pa). The IR spectra of tholin formed at around 130 Pa by Coll et al. (1999) appears to be close to our tholin formed at 160 Pa, although they use different ratio of CH_4/N_2 ($= 2/98$) for the initial gas mixture. Although these previous studies use different energy sources and initial gas mixture from our studies, tholins formed almost at the same pressure show similar infrared spectra. Thus, the deposition pressure appears to a very important factor controlling the tholin-forming reactions.

It has been rather controversial whether tholin contains a significant amount of aromatic macromolecules or not. While nitrogen-containing heteroaromatics and PAHs were detected in tholin formed at Cornell University (Khare et al., 1984b; Sagan et al., 1993; Ehrenfreund et al., 1995), Coll et al., (1999) could not find any aromatic compounds except benzene in their tholin. We have shown that the amount of aromatic and heteroaromatic rings is greater in tholin formed at lower pressures. It is possible that this pressure effect on the amount of aromatic compounds is one of the main reasons for the discrepancy between these previous studies (Khare et al., 1984b; Coll et al., 1999).

The k-values at UV/VIS wavelengths are compared with previous work in Fig. 14. Good agreement of k-values in both magnitude and slope is found between Khare et al. (1984a) and our tholins formed at 13 and 26 Pa. The k-values reported by Ramirez et al. (2002) for a tholin formed from a $CH_4/N_2 = 2/98$ mixture in a DC glow discharge at 130 Pa are between the k-values of our tholins formed at 160 and 2300 Pa. The slight discrepancy may come from the difference in the amount of CH_4 in the initial gas mixture. Nevertheless, the k-values in tholins formed at more than 100 Pa are about 10 times smaller than those of Khare et al. (1984a). The comparison of optical properties of tholin in the UV/VIS range also indicates that pressure is one of the major factors in tholin production processes. The larger absorption in UV/VIS is very consistent with the larger amount of aromatic macromolecules in tholin formed at lower pressures.

The k-values of Uranus tholin formed from a CH_4/H_2 gas mixture without nitrogen (Khare et al., 1987) is close to that of our 2300 Pa tholin (Table 4), which has the highest C/N ratio among our tholins. These results suggest that the nitrogen incorporation into tholin could increase the k-value in visible wavelength, in agreement with suggestions by Scattergood and Owen (1977). The increases in absorption in longer wavelength at visible light could be enhanced by the unpaired electrons of nitrogen interacting with the delocalized π electrons from aromatics (e.g., Rao, 1975).

The ratios of C/N and C/H measured in this study are compared to previous work in Fig. 15. The C/N ratio of our tholins at 26–160 Pa are close to the tholin formed by DC glow discharge at 20 Pa (Sagan et al., 1984). The C/N ratio of 2.8 for tholin formed by DC glow discharge from $CH_4/N_2 = 2/98$ gas mixture at a low temperature and a pressure of ~ 200 Pa (Coll et al., 1999) is close to the C/N ratio for our tholin at 2300 Pa. The value of $C/N = 2.8$ (Coll et al., 1999) is slightly higher than the value of $C/N = 2$ at 160 Pa, even when Coll et al. (1999) conducted an experiment at a similar pressure but with a $CH_4/N_2 = 2/98$ gas mixture with less CH_4 than our initial gas mixture of $CH_4/N_2 = 10/90$. This slight difference may be due to the effect of low temperature and is probably not due to the difference of CH_4/N_2 ratio in the initial gas mixture. Although the causes of the differences in elemental compositions are not yet understood, the C/N ratio is very sensitive to the experimental conditions.

The C/N ratios of tholins produced at the pressure less than 200 Pa appear to be in the range from 1.5 to 3. The tholins formed by spark discharge at around 10^5 Pa have a C/N ratio of 5.5 (McKay, 1996) to 11 (Coll et al., 1995).

Table 4
Tholin synthesized by an electrical discharge

Reference	Pressure	Initial gasmixture	Discharge	Temperature	System	k-value at 0.5 μm	C/N	C/H	Chemical properties
Khare et al. (1984a)	20 Pa	10% CH_4, 90% N_2	DC glow	300 K	Flow	0.04	1.94[a]	0.6[a]	Less aliphatic C–H, amines, nitriles (IR)
									Aromatics and N heteroaromatics (Py-GC/MS)[b]
									2–4 rings PAHs (L^2MS)[c]
Khare et al. (1987)	13 Pa	100% CH_4	RF glow	300 K	Flow	0.00108–0.00375		0.71[d]	Aliphatic C–H, (N–H or O–H due to leak?) (IR)
	13 Pa	7% CH_4, 93% H_2	RF glow	300 K	Flow	0.0014–0.0027		0.66[d]	
	13 Pa	3% CH_4, 25% He, 72% H_2	RF glow	300 K	Flow	0.0044–0.035		0.57[d]	No CH, 1050 cm^{-1} (Si-O, glass contamination?) (IR)
McDonald et al. (1994)	200 Pa	10% CH_4, 90% N_2	RF glow	300 K	Flow		1.5[e]	0.6[e]	Aliphatic C–H, amines, nitriles, double bonds (IR)
	100 Pa	0.1% CH_4, 99.9% N_2	RF glow	300 K	Flow		0.75	0.6	No nitriles, weak C–H, amines, double bonds (IR)
Coll et al. (1995)	90000 Pa	11% CH_4, 89% N_2	Spark	∼ 100 K	Closed[f]		11	1	
McKay (1996)	10^5 Pa	10% CH_4, 90% N_2	Spark	300 K	Flow		5.5	1	
Coll et al. (1999)	∼ 200 Pa	2% CH_4, 98% N_2	DC glow	100–150 K	Flow		2.8	0.8	Aliphatic C–H, amines, nitriles (IR)
									No aromatic except benzene (Py-GC/MS)
Ramirez et al. (2002)	∼ 100 Pa	2% CH_4, 98% N_2	DC glow	300 K	Flow	0.0034			
Khare et al. (2002)	7100 Pa	10% CH_4, 90% N_2	RF discharge	300 K	Closed[g]				Aliphatic C–H, amines, nitrile double bonds, rings (IR)
This study	13 Pa	10% CH_4, 90% N_2	RF glow	300 K	Flow	0.031	1.45	0.75	No aliphatic C–H, amines, nitriles (IR), abundant aromatics[h]
	26 Pa	10% CH_4, 90% N_2	RF glow	300 K	Flow	0.032	1.78	0.80	Less aliphatic C–H, amines, nitriles (IR), abundant aromatics[h]
	67 Pa	10% CH_4, 90% N_2	RF glow	300 K	Flow	0.014	1.85	0.80	Aliphatic C–H, amines, nitriles (IR), abundant aromatics[h]
	160 Pa	10% CH_4, 90% N_2	RF glow	300 K	Flow	0.0047	1.97	0.79	Aliphatic C–H, amines, nitriles (IR), less aromatics[h]
	2300 Pa	10% CH_4, 90% N_2	RF glow	310 K	Flow	0.0018	2.76	0.73	Aliphatic C–H, amines, nitriles (IR), much less aromatics[h]

[a] Sagan et al. (1984).
[b] Khare et al. (1984b), Ehrenfreund et al. (1995).
[c] Sagan et al. (1993).
[d] Elemental analysis (Khare, unpublished data).
[e] Data from Sagan et al. (1984).
[f] CH_4 partial pressure maintained as 1300 Pa.
[g] Periodic supply of N_2/CH_4 for every 2 hr.
[h] Abundance and size of aromatics are inferred from IR and UV/VIS spectroscopy, Raman spectroscopy, μL^2MS.

These high C/N ratios suggest that carbon is incorporated easily into tholin in a hot plasma. The dominant chemical processes in cold plasma and hot plasma may be considerably different. Titan's haze might have different C/N ratios not only due to the difference in altitude, but also due to the formation mechanisms, such as charged particle irradiation (cold plasma) and meteor impact/lightning (hot plasma), although the latter is unlikely to be a major effect in haze formation processes.

Solid products produced by proton irradiation (2.5 MeV, Scattergood and Owen, 1977) and by UV irradiation (Khare and Sagan, 1973; Podolak et al., 1979; Bar-Nun et al., 1988; Scattergood et al., 1992; Clarke and Ferris, 1997) in simulated planetary atmospheres have been studied previously. The optical properties of poly-C_2H_2, poly-C_2H_4, and poly-HCN (Podolak et al., 1979; Bar-Nun et al., 1988) poorly match Titan tholin (Khare et al., 1984a) and are unlikely to be a major constituent of the Titan haze (Khare et al., 1994). Recently, the optical constants of the polymer produced by UV irradiation were measured (Tran et al., 2003). A simulated "Titan gas mixture" (N_2: 0.98, CH_4: 0.018, H_2: 0.002, C_2H_2: 3.5×10^{-4}, C_2H_4: 3.5×10^{-5}, HC_3N: 1.7×10^{-5}) was irradiated with the 185 and 254 nm UV irradiation at 93100 and 13300 Pa. The derived k-value in UV/VIS range is close to (or even higher than) that of Khare et al. (1984a). The C/N ratio was around 18. This high C/N ratio would be partially due to their initial gas mixture, especially without HCN. Although the C/H ratio was not mentioned, it is suggested that the significant amount of hydrogen would be included in their polymer because of the intense IR absorptions of the aliphatic C–H bands. Although the IR spectrum of the UV polymer is close to our tholin formed at 2300 Pa rather than those formed at 26 Pa, the k-value is much larger than the k-value of our tholin formed at 2300 Pa. This discrepancy remains to be explained.

4.4. Application to Titan

In Section 4.1 we suggested the presence of the clusters of nitrogen-containing polycyclic aromatic compounds (N-PACs) in tholin formed at low pressures. In this section, we discuss the implications of our laboratory results to Titan's haze, and their role in Titan's atmospheric thermal structure and complex organic chemistry.

4.4.1. Comparison with Titan's observations

The visible region of Titan's geometric albedo between 0.3 and 0.6 μm is determined mainly by the optical properties of the haze (McKay et al., 2001). In this visible region, the k-values of Titan's haze inverted from the geometric albedo (Rages and Pollack, 1980; McKay et al., 1989; McKay and Toon, 1992) were similar in form to those of Titan tholin measured by Khare et al. (1984a, 1984b) (Fig. 16). This reasonable agreement (within a factor of 2) leads to the assumption that the optical properties of Titan haze would be represented by the laboratory Titan tholin multiplied by an adjustable correction factor (McKay et al., 1989; McKay and Toon, 1992). McKay et al. (1989) reported that the best fit to the Titan's geometric albedo was obtained if the k-values of Titan tholin (Khare et al., 1984a) were multiplied by a factor of 1.33. Our new k-values of tholins formed at 13 and 26 Pa agree well with those of Khare et al. (1984a) (Fig. 14). Thus, the k-values of tholin formed at lower pressures would account for the observed geometric albedo of Titan more readily than those formed at higher pressures.

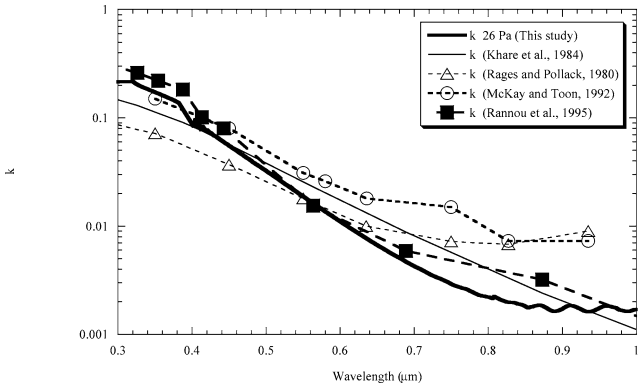

Fig. 16. The k-values of tholin are shown, along with the k-values deduced from the haze models (Mie particles) to fit the observed Titan's geometric albedo by Rages and Pollack (1980) (triangles) and McKay and Toon (1992) (circles). The k-values consistent with observations are also shown for the "fractal" aerosol model (fractal dimension = 2, production height = 535 km) (Rannou et al., 1995) (full squares).

Titan's observed geometric albedo has been explained reasonably well with various microphysical/radiative models (McKay et al., 1989; Courtin et al., 1991; Toon et al., 1992; Rannou et al., 1995), which assume aerosols with the optical properties similar to be the laboratory tholin of Khare et al. (1984a) multiplied by correction factors. The comparison between model and observation may not be fine enough to distinguish the fine structure of the variation of the optical properties with wavelength (McKay and Toon, 1992). Nonetheless, it is interesting to note that our new k-values of tholin formed at 26 Pa agree well with one of the k-values deduced from the recent "fractal" aerosol model (fractal dimension = 2, production height = 535 km) (Rannou et al., 1995) which needs slightly larger k-values in the UV region than those of Khare et al. (1984a) (Fig. 16).

The C/N ratio of tholin is another piece of supporting evidence that tholin formed at low pressure would be a good representation of Titan's haze. From a detailed photochemical model, Lara et al. (1996) showed the difficulty in simultaneously reproducing the observed mixing ratios of the C_2 hydrocarbons in the lower stratosphere (Coustenis et al., 1989) and the observed HCN vertical distribution (Tanguy et al., 1990; Hidayat et al., 1998; Marten et al., 2002) with a single eddy diffusion profile. Lara et al. (1999) took into account a loss of HCN into the haze with a simple parameterization and simultaneously reproduced the observed HCN and C_2 hydrocarbons in the lower stratosphere. The calculated C/N ratio in Titan's haze was 1.7–2.0, which is

in agreement with the C/N ratio of 1.5–1.8 obtained from tholin formed at 13–26 Pa.

These agreements both in optical properties and in the C/N ratio suggest that tholin formed at low pressures (13 and 26 Pa) would be a good representation of the Titan's haze. This suggests the presence of nitrogen-containing polycyclic aromatic compounds (N-PACs) in Titan's haze. Titan's haze would contain a large amount of nitrogen with a C/N ratio in the range of 1.5 to 1.8 and a C/H ratio in the range of 0.75–0.8, which would be an important sink for both nitrogen and hydrogen in its atmosphere.

The good agreement with tholin formed at lower pressures and observed geometric albedo of Titan is very consistent with the good agreement between Titan's atmospheric composition and the gas products formed at low pressure (Thompson et al., 1991). The gas product distributions produced by cold plasma at 24 and 1700 Pa were determined by GC/MS (Thompson et al., 1991). They found that the gas products formed at 24 Pa contained a significant amount of unsaturated hydrocarbons and nitriles. Except for the primarily photochemical products (C_2H_6 and C_3H_8), the gas product distribution at low pressure (24 Pa) explains the minor constituents detected by Voyager in Titan's atmosphere much better than those formed at higher pressure (1700 Pa), since the gas products of 1700 Pa contained less amounts of unsaturated hydrocarbons (Thompson et al., 1991). The good agreement for both the gas products distribution and the optical properties of tholin at low pressures with Titan's observations suggest that our laboratory simulations by cold plasma at low pressures represent reasonably well the complex organic chemistry in Titan's atmosphere.

The relatively good agreement in the k-values of tholin formed at low pressures (13–26 Pa) with the observed geometric albedo suggest that the haze would be mainly formed at the altitudes higher than 200 km ($\sim 10^2$ Pa). Microphysical models (McKay et al., 1989; Rannou et al., 1995) suggest that the main production of haze around 10^{-2} Pa (600 km) is consistent with the Titan's observed geometric albedo and the haze extinction profile (Rages and Pollack, 1983). Recently, Rannou et al. (1997) have shown that the haze formation altitude would not be as high as 535 km but around 385 km to fit the Voyager's high phase angle images. Our experiments are generally consistent with a high altitude for the formation of the haze (pressure less than ~ 10 Pa) but we cannot distinguish between the specific heights suggested above because of the lack of the reliable simulations at pressure lower than 10 Pa.

The unsaturated compounds in Titan's atmosphere, such as HCN, C_2H_2, C_2H_4, C_3H_4, C_4H_2, HC_3N, and C_2N_2, were observed to be enriched at high latitudes in the northern hemisphere, when the northern hemisphere was in the spring season at the time of Voyager 1 encounter (Coustenis and Bezard, 1995). Rannou et al. (1997) suggests that the k-value at 0.5 μm could increase around the Titan's north pole. In a laboratory simulation, unsaturated gas compounds are formed at lower pressures more readily than at higher pressures in a cold plasma (Thompson et al., 1991). Experiments in this study also show that the aromatic compounds are more abundant in tholin formed at lower pressures than in those formed at high pressures. If the higher concentration of unsaturated gas compositions around Titan's north pole leads to the higher abundance of aromatic compounds in Titan's haze, the k-values in the UV/VIS range would be increased like tholin formed at lower pressures. It is interesting to note that HCN is 23 times more abundant in the north than in the south (Coustenis and Bezard, 1995). This enrichment of HCN gas could promote the incorporation of nitrogen in haze particles, forming nitrogen-containing polycyclic aromatic compounds (N-PACs).

The microphysical/radiative models (McKay et al., 1989; Toon et al., 1992; Rannou et al., 1995, 1997) assume that the aerosols have an altitude-independent composition with optical properties similar to the laboratory tholin (Khare et al., 1984a). However, our study suggests that the aerosols might have different chemical/optical properties at different altitudes, as proposed by Chassefiere and Cabane (1995) based on theoretical considerations. Haze particles formed at higher altitudes could be covered by the transparent materials (in the visible range) formed at lower altitudes, which would lead to the variation of optical properties of haze at different altitudes. The variation in chemical and optical properties with altitude needs to be taken into consideration in future modeling.

4.4.2. Implication of nitrogen-containing polycyclic aromatic compounds (N-PACs) for Titan's atmosphere

The presence of the nitrogen-containing polycyclic aromatic compounds (N-PACs) in Titan's haze may have significant implications for Titan's atmosphere. Because those aromatic macromolecules are efficient absorbers of UV/VIS light, they may control the optical properties of Titan's haze, thereby dominating the thermal structure of Titan's atmosphere (e.g., McKay et al., 1989, 1991). The presence of aromatic macromolecules also affects the charge state of haze by the UV photoelectric ejection processes (Bakes et al., 2002). The charging strongly influences haze coagulation processes and hence may change the optical properties of haze by controlling their size distribution (Bakes et al., 2002).

N-PACs may play an important role in converting simple molecules to haze particles in Titan' atmosphere, since nitrogen atoms in the ring promote the formation of an additional ring (Ricca et al., 2001). These aromatic macromolecules are efficient charge exchange intermediaries and may play a central role in gas phase chemistry (Bakes and Tielens, 1994, 1998). Aromatic macromolecules in Titan haze might remove highly reactive hydrogen atoms as hydrogen molecules through the catalytic reactions on the aerosol surfaces (Yung et al., 1984; Courtin et al., 1991; Bakes et al., 2003; Lebonnois et al., 2003).

The strong hydrogen bonding caused by nitrogen-containing heteroaromatics could be important as sites for gas

adsorption on the surface of tholin. Preliminary analysis with IR spectroscopy suggests that the substantial amounts of NH_3 and HCN were degassed from the surface of tholin that was formed and kept under vacuum. Tholin may adsorb these gases on its surface, possibly by the interaction of hydrogen bonds. This implies that Titan's haze could adsorb NH_3 and HCN on the particle surfaces and could carry these gases from higher altitudes to the lower atmosphere of Titan where condensation occurs. These adsorbed molecules could thus be an important source of nitrogen in the lower atmosphere and at the surface of Titan.

5. Conclusions

We have conducted laboratory simulations of Titan tholin using cold plasma at various pressures in $CH_4/N_2 = 10/90$ gas mixture. The experimental results indicate that chemical and optical properties of the resulting tholin depend on the deposition pressure (13–2300 Pa) in cold plasma. Based on our results we suggest the following conclusions:

(1) Both the amount and size of aromatic ring compounds in tholin increase as deposition pressure decreases.
(2) The abundance of saturated C–H bonds is lower in tholin formed at low pressures, while N–H bonds become more abundant.
(3) More nitrogen is included in carbon networks at lower pressures, such as carbon diimides (–N=C=N–) and isocyanides (–C–N≡C). In contrast, at higher deposition pressures, nitrogen exists as a terminal group, such as nitrile (–C≡N).
(4) Tholins formed at low pressures contain the clusters of nitrogen-containing polycyclic aromatic compounds (N-PACs) in a matrix of carbon and nitrogen branched chain networks, which are connected tightly to each other with hydrogen bonding of N–H bonds. Tholin formed at high pressure (2300 Pa) consists of a polymer-like branched chain structure terminated with $–CH_3$, $–NH_2$, and –C≡N with fewer aromatic compounds.
(5) The carbon/nitrogen ratio in tholins increases from a value between 1.5 and 2 at lower pressures to 3 at a high pressure (2300 Pa). This indicates that nitrogen is incorporated into tholin more efficiently at lower deposition pressures.
(6) Reddish-brown tholin films formed at low pressures (13 and 26 Pa) showed stronger UV/VIS absorptions than yellowish tholin films formed at high pressures (160 and 2300 Pa). The imaginary part of the optical constant (k-value) at UV/VIS wavelengths depends strongly on the delocalized π electrons from aromatics and nitrogen heteroaromatic compounds in tholins.

Applying the experimental results to Titan, we suggest that the tholins formed at low pressures (13 and 26 Pa) may be better representations of Titan's haze than those formed at high pressures (160 and 2300 Pa). This is because the optical properties of tholin formed at low pressures agree well with that of Khare et al. (1984a, 1984b), which have been shown to account for the Titan's observed geometric albedo (McKay et al., 1989). Thus, the nitrogen-containing polycyclic aromatic compounds (N-PACs) that we find in tholin formed at low pressure may be present in Titan's haze. These aromatic macromolecules may have a significant influence over the thermal structure and complex organic chemistry in Titan's atmosphere, because they are efficient absorbers of UV radiation and efficient charge exchange intermediaries. The pressure effect on the chemical and optical properties of tholins suggests that the haze layers at various altitudes might have different chemical and optical properties. These variations of chemical and optical properties as a function of altitude will be investigated by the Cassini/Huygens mission beginning in 2004.

Acknowledgments

This work was supported by NASA Exobiology Grant NCC2-1118, NCC2-1358, and NASA Cosmochemistry Program NAG5-12673. H.I. was also supported partially by the Japanese Scientific Foundation. The Nicolet Corporation is acknowledged for use of the Raman spectrometer. The Center of Nanotechnology in NASA Ames Research Center is acknowledged for use of the UV/VIS spectrometer. We are grateful to Dr. Ralph Lorenz and Dr. Gene McDonald for helpful reviews. Dr. Louis Allamondola and Dr. Max Bernstein are acknowledged for the useful discussions of Raman and infrared spectra. H.I. thanks Dr. Tom Frey for carefully reading the manuscript and giving useful comments. Dr. Warren Belisle is acknowledged for conducting the elemental analysis. Mr. Jeff Ifland is acknowledged for technical assistance with the plasma chamber.

Appendix A. Characteristic frequencies and assignments in infrared spectra

The characteristic frequencies and the detailed peak assignments of the IR spectra of tholins in this study (Rao, 1963; Bellamy, 1975, 1980, Colthup et al., 1990; Lin-Vien et al., 1991; Socrates, 2001) are described here (Fig. 3, Table 2).

Three peaks around 2900 cm^{-1} (3.45 μm) in tholins are assigned to saturated C–H stretch vibrations. The absorptions at ∼ 2960 and ∼ 1460 cm^{-1} (3.38 and 6.85 μm) correspond to $–CH_3$ antisymmetric stretching and bending, respectively. The absorptions at ∼ 2873 and ∼ 1375 cm^{-1} (3.48 and 7.27 μm) correspond to $–CH_3$ symmetric stretching and umbrella bending, respectively. The peak at ∼ 2930 cm^{-1} (3.41 μm) is assigned to $–CH_2–$ antisymmetric stretching. The very weak peak at 2730 cm^{-1} (3.66 μm)

is tentatively assigned to methyl/methylene groups attached to nitrogen (–N–CH_3, –N–CH_2–).

Two or three peaks around 3200–3500 cm^{-1} (3.13–2.86 μm) are likely due to N–H stretch vibrations by amines. In general, aliphatic primary amines (R–NH_2) have two N–H stretching bands, the antisymmetric stretching (3350–3400 cm^{-1}, (2.99–2.94 μm)) and the symmetric stretching (3280–3350 cm^{-1}, (3.05–2.99 μm)). The weak doublet at 3360 and 3320 cm^{-1} (2.98 and 3.01 μm) is observed only in tholins formed at 2300 and 160 Pa and is assigned to the N–H stretchings of the primary amines (R–NH_2). Aliphatic secondary amines (R–NH–R) have also a N–H stretching band around 3300 cm^{-1} (3.03 μm). The broad peak around 3350 cm^{-1} (2.99 μm) in tholins is probably due to the –NH_2 symmetric stretching and the –NH– stretching of amines. The characteristic peak of imines (>C=N–H) is also consistent with the observed broad 3300 cm^{-1} (3.03 μm) band in tholins. The peak around 3200 cm^{-1} (3.13 μm) in tholins is probably due to –NH– stretching bands, which is shifted to lower frequencies by hydrogen bond interactions (Lin-Vien et al., 1991). This peak at 3200 cm^{-1} may also be caused from overtone from –NH_2 scissors bending enhanced by Fermi resonance interactions with the –NH_2 symmetric stretchings (Lin-Vien et al., 1991). The two major peaks at 3350 and 3200 cm^{-1} (2.99 and 3.13 μm) are also observed in the previous Titan tholin (McDonald et al., 1994). Aromatic amines have characteristic frequencies of –NH_2 stretching bands larger than those of aliphatic amines (Lin-Vien et al., 1991). The shoulder around 3460 cm^{-1} (2.89 μm) in tholin may be due to aromatic amines.

It is well known that the NH stretching bands are broadened due to hydrogen bonding caused by their polar N–H bonds (Bellamy, 1980; Colthup et al., 1990; Lin-Vien et al., 1991). Further, the effect of hydrogen bonds increases the intensity and lowers the frequency of N–H stretching bands (Bellamy, 1980; Lin-Vien et al., 1991). These polar N–H bonds cause a wide variety of hydrogen bonding, including the usual NH—lone-pair or π-electrons type hydrogen bonding. A broad absorption in the region of 3200–2700 cm^{-1} (3.13–3.70 μm) is characteristic to many secondary heteroaromatic amines, such as pyrazoles and indazoles, which contain more than one nitrogen atom in the aromatic ring. This broadening is caused by the hydrogen bonding between the N–H bonds and the unsaturated N atom of the heterocyclic rings (Bellamy, 1980; Lin-Vien et al., 1991).

The broad absorptions at 3200–3500 cm^{-1} (3.13–2.86 μm) in Fig. 3 suggest that hydrogen bonds caused by N–H bonds are predominant in Titan tholins. The extension of N–H bands to frequencies lower than 2600 cm^{-1} (3.85 μm) may be caused by the strong hydrogen bonds between N–H moieties and the unsaturated N atom of the heterocyclic ring. It is also interesting to note that amine salts exhibit a series of IR bands in the 2800–2100 cm^{-1} region (Lin-Vien et al., 1991). Thus, the existence of amine salts in tholin cannot be excluded.

The peaks around 1600 cm^{-1} (6.25 μm) are probably caused by (1) NH_2 scissors bending (primary amines) and/or (2) aromatics, and/or (3) C=N groups, and/or (4) the conjugated double bonds (C=C) of alkenes with phenyl (C=C–Ph) or nitrile groups (C=C–C≡N).

Primary amines (–NH_2) show strong absorption bands in the region from 1638 to 1590 cm^{-1} (6.11–6.29 μm).

Aromatic rings show characteristic frequencies in the 1620–1565 cm^{-1} (6.17–6.39 μm) regions. In mono- and di-substituted benzenes, the ring stretch components (two quadrant stretch vibrations) usually give rise to bands at 1620–1585 cm^{-1} (6.17–6.31 μm) and 1590–1565 cm^{-1} (6.29–6.39 μm) (Lin-Vien et al., 1991). The second band is often weaker in the IR than the first, but is sometimes enhanced by ring conjugation (Lin-Vien et al., 1991; Socrates, 2001). Heteroaromatics that contain nitrogen also show characteristic frequencies in this region (Socrates, 2001). The symmetric ring vibration (E_{2G2}, G-band) around 1580 cm^{-1} (6.33 μm) would be activated by the break of symmetry due to nitrogen incorporation (Kaufman et al., 1989).

The stretching bonds of C=C in alkenes occur between 1680 and 1635 cm^{-1} (5.95 and 6.12 μm). In general, conjugation between C=C bonds and C≡N moieties results in a lowering of the C=C stretching frequency. The presence of a C≡N group adjacent to C=C double bonds enhances the IR intensity of the C=C stretching mode (Lin-Vien et al., 1991). The Schiff bases (C_2C=N–), guanidine (N_2C=N–), amidines (N–C=N) and azines (>C=N–N=C<) all show C=N bond vibrations around 1600–1670 cm^{-1} (6.25–5.99 μm) (Colthup et al., 1990). Thus the peak around 1630 cm^{-1} (6.13 μm) suggests the prescence of the C=N and C=C bonds conjugated with each other, and with the C≡N and phenyl groups.

The peaks around 2100–2300 cm^{-1} (4.76–4.35 μm) in tholins are caused by triple bonds (C≡N and C≡C) and cumulative double bonds (such as N=C=N). These peaks are probably aliphatic nitriles (2240 cm^{-1}, (4.46 μm)), aromatic nitriles (2210, 2230 cm^{-1}, (4.52, 4.48 μm)), carbon diimide or aliphatic isocyanide (2150 cm^{-1}, (4.65 μm)), aryl isocyanide (2135 cm^{-1}, (4.68 μm)), and ketene imines or diazo compounds (2100 cm^{-1}, (4.76 μm)). The large peak at 2180 cm^{-1} (4.59 μm) may be due to conjugated nitriles. It is known that conjugation of C≡N to C=C groups lowers its frequency to 2235–2215 cm^{-1} (4.47–4.51 μm) and may shift to lower values in the presence of a strong electron-donating group, such as an amino moiety (–NH_2 or –NR_2), on the β-carbon of the double bond (Lin-Vien et al., 1991). C≡N bands are also broadened and enhanced by the conjugated group in the majority of cases. Thus, the peak at 2180 cm^{-1} (4.59 μm) in tholin suggest the presence of conjugated structures, such as –(NH_2)C=C(–C≡N)–.

Asymmetric and symmetric –CH_3 bending have characteristic frequencies around 1460 and 1380 cm^{-1} (6.85 and 7.25 μm), respectively. These two peaks are observed in tholins formed at high pressures. The weak shoulder at

1424 cm^{-1} (7.02 μm) is probably due to $=CH_2$ scissors bending. The relatively broad peak observed around 1440–1450 cm^{-1} (6.94–6.90 μm) in tholins formed at low pressures is assigned to the ring stretching of aromatics. The peak at 980 cm^{-1} (10.2 μm) is probably due to vinyl C–H bending. The peak at 818 cm^{-1} observed in tholins formed at low pressures is assigned to the C–H wag of aromatics. The broad peaks around 1150 and 850 cm^{-1} (8.70 and 11.8 μm) may be due to aromatic and aliphatic C–N bending. The "skeletal ring vibration" at 1350 cm^{-1} (7.4 μm) (Khare et al., 2002) was not detected in this study.

References

Bakes, E.L.O., Tielens, A.G.G.M., 1994. The photoelectric heating mechanism for very small graphitic grains and polycyclic aromatic hydrocarbons. Astrophys. J. 427, 822–838.

Bakes, E.L.O., Tielens, A.G.G.M., 1998. The effects of polycyclic aromatic hydrocarbons on the chemistry of photodissociation regions. Astrophys. J. 499, 258–266.

Bakes, E.L.O., McKay, C.P., Bauschlicher, J.C.W., 2002. Photoelectric charging of submicron aerosols and macromolecules in the Titan haze. Icarus 157, 464–475.

Bakes, E.L.O., Lebonnois, S., Bauschlicher, J.C.W., McKay, C.P., 2003. The role of submicrometer aerosols and macromolecules in H_2 formation in the Titan haze. Icarus 161, 468–473.

Bar-Nun, A., Kleinfeld, I., Ganor, E., 1988. Shape and optical properties of aerosols formed by photolysis of acetylene, ethylene, and hydrogen cyanide. J. Geophys. Res. 93, 8383–8387.

Bellamy, L.J., 1975. The Infra-red Spectra of Complex Molecules, third ed. Chapman and Hall, London. 433 p.

Bellamy, L.J., 1980. Advances in Infrared Group Frequencies, second ed. Chapman and Hall, London. 299 p.

Bernstein, M.P., Sanford, S.A., Allamondola, L.J., 1997. The infrared spectra of nitriles and related compounds frozen in Ar and H_2O. Astrophys. J. 476, 932–942.

Chassefiere, E., Cabane, M., 1995. Two formation regions for Titan's hazes: indirect clues and possible synthesis mechanism. Planet. Space Sci. 43, 91–103.

Clarke, D.W., Ferris, J.P., 1997. Titan haze: structure and properties of cyanoacetylene and cyanoacetylene–acetylene photopolymers. Icarus 127, 158–172.

Clemett, S.J., Zare, R.N., 1997. Microprobe two-step laser mass spectrometry as an analytical tool for meteoritic samples. In: Dishoeck, E.F.V. (Ed.), Molecules in Astrophysics: Probes and Processes. Kluwer Academic, Dordrecht, pp. 305–320.

Coll, P., Coscia, D., Gazeau, M.-C., de Vanssay, E., Guillemin, J.C., Raulin, F., 1995. Organic chemistry in Titan's atmosphere: new data from laboratory simulations at low temperature. Adv. Space Res. 16, 93–103.

Coll, P., Coscia, D., Smith, N., Gazeau, M.-C., Ramirez, S.I., Cernogora, G., Israel, G., Raulin, F., 1999. Experimental laboratory simulation of Titan's atmosphere: aerosols and gas phase. Planet. Space Sci. 47, 1331–1340.

Colthup, N.B., Daly, L.H., Wiberley, S.E., 1990. Introduction to Infrared and Raman Spectroscopy, third ed. Academic Press, San Diego.

Courtin, R., Wagener, R., McKay, C.P., Caldwell, J., Fricke, K.-H., Raulin, F., Bruston, P., 1991. UV spectroscopy of Titan's atmosphere, planetary organic chemistry and prebiological synthesis. II. Interpretation of new IUE observations in the 235–335 nm range. Icarus 90, 43–56.

Courtin, R., Gautier, D., McKay, C.P., 1995. Titan's thermal emission spectrum: reanalysis of the Voyager infrared measurements. Icarus 114, 144–162.

Coustenis, A., Bezard, B., 1995. Titan's atmosphere from Voyager infrared observations. IV. Latitudinal variations of temperature and composition. Icarus 115, 126–140.

Coustenis, A., Bezard, B., Gautier, D., 1989. Titan's atmosphere from Voyager infrared observations I. The gas composition of Titan's equatorial region. Icarus 80, 54–76.

Denaro, A.R., Jayson, G.G., 1972. Fundamentals of Radiation Chemistry. Butterworth, London.

Ehrenfreund, P., Boon, J.J., Commandeur, J., Sagan, C., Thompson, W.R., Khare, B., 1995. Analytical pyrolysis experiments of Titan aerosol analogues in preparation for the Cassini–Huygens mission. Adv. Space Res. 15, 335–342.

Ferrari, A.C., Robertson, J., 2000. Interpretation of Raman spectra of disordered and amorphous carbon. Phys. Rev. B 61, 14095–14107.

Hanel, R., Conrath, B., Flasar, F.M., Kunde, V., Maguire, W., Pearl, J., Pirraglia, J., Samuelson, R., Herath, L., Allison, M., Cruikshank, D., Gautier, D., Gierasch, P., Horn, L., Koppany, R., Ponnamperuma, C., 1981. Infrared observations of the saturnian system from Voyager 1. Science 212, 192–200.

Hanel, R., Conrath, B., Flasar, F.M., Kunde, V., Maguire, W., Pearl, J., Pirraglia, J., Samuelson, R., Cruikshank, D., Gautier, D., Gierasch, P., Horn, L., Ponnamperuma, C., 1982. Infrared observations of the saturnian system from Voyager 2. Science 215, 544–548.

Hidayat, T., Marten, A., Bezard, B., Gautier, D., Owen, T., Matthews, H.E., Paubert, G., 1998. Millimeter and submillimeter heterodyne observations of Titan: retrieval of the vertical profile of HCN and the $^{12}C/^{13}C$ ratio. Icarus 126, 170–182.

Hunten, D.M., Tomasko, M.G., Flasar, F.M., Samuelson, R.E., Strobel, D.F., Stevenson, D.J., 1984. Titan. In: Gehrels, T., Matthews, M.S. (Eds.), Saturn. Univ. of Arizona Press, Tucson, pp. 671–759.

Kaufman, J.H., Metin, S., Saperstein, D.D., 1989. Symmetry breaking in nitrogen-doped amorphous carbon: infrared observation of the Raman-active G and D bands. Phys. Rev. B 39, 13053–13060.

Khare, B.N., Sagan, C., 1973. Red clouds in reducing atmospheres. Icarus 20, 311–321.

Khare, B.N., Sagan, C., Zumberge, J.E., Sklarew, D.S., Nagy, B., 1981. Organic solids produced by electrical discharge in reducing atmospheres: tholin molecular analysis. Icarus 48, 290–297.

Khare, B.N., Sagan, C., Arakawa, E.T., Suits, F., Callcott, T.A., Williams, M.W., 1984a. Optical constants of organic tholins produced in a simulated titanian atmosphere: from soft X-ray to microwave frequencies. Icarus 60, 127–137.

Khare, B.N., Sagan, C., Thompson, W.R., Arakawa, E.T., Suits, F., Callcott, T.A., Williams, M.W., Shrader, S., Ogino, H., Willingham, T.O., Nagy, B., 1984b. The organic aerosols of Titan. Adv. Space Res. 4, 59–68.

Khare, B.N., Sagan, C., Thompson, W.R., Arakawa, E.T., Votaw, P., 1987. Solid hydrocarbon aerosols produced in simulated uranian and neptunian stratospheres. J. Geophys. Res. 92, 15067–15082.

Khare, B.N., Sagan, C., Thompson, W.R., Arakawa, E.T., Meisse, C., Tuminello, P.S., 1994. Optical properties of poly-HCN and their astronomical applications. Can. J. Chem. 72, 678–694.

Khare, B.N., Bakes, E.L.O., Imanaka, H., McKay, C.P., Cruikshank, D.P., Arakawa, E.T., 2002. Analysis of the time-dependent chemical evolution of Titan haze tholin. Icarus 160, 172–182.

Krimigis, S.M., Armstrong, T.P., Axford, W.I., Bostrom, C.O., Gloeckler, G., Keath, E.P., Lanzerotti, L.J., Carbary, J.F., Hamilton, D.C., Roelof, E.C., 1981. Low-energy charged particles in Saturn's magnetosphere: results from Voyager 1. Science 212, 225–231.

Krimigis, S.M., Armstrong, T.P., Axford, W.I., Bostrom, C.O., Gloeckler, G., Keath, E.P., Lanzerotti, L.J., Carbary, J.F., Hamilton, D.C., Roelof, E.C., 1982. Low-energy hot plasma and particles in Saturn's magnetosphere. Science 215, 571–577.

Kunde, V.G., Aikin, A.C., Hanel, R.A., Jennings, D.E., Maguire, W.C., Samuelson, R.E., 1981. C_4H_2, HC_3N and C_2N_2 in Titan's atmosphere. Nature 292, 686–688.

Lara, L.-M., Lellouch, E., Lopez-Moreno, J.J., Rodrigo, R., 1996. Vertical distribution of Titan's atmospheric neutral costituents. J. Geophys. Res. 101, 23261–23283.

Lara, L.-M., Lellouch, E., Shematovich, V., 1999. Titan's atmospheric haze: the case for HCN incorporation. Astron. Astrophys. 341, 312–317.

Lara, L.-M., Banaszkiewicz, M., Rodrigo, R., Lopez-Moreno, J.J., 2002. The CH_4 density in the upper atmosphere of Titan. Icarus 158, 191–198.

Lebonnois, S., Bakes, E.L.O., McKay, C.P., 2003. Atomic and molecular hydrogen budget in Titan's atmosphere. Icarus 161, 474–485.

Lellouch, E., Coustenis, A., Gautier, D., Raulin, F., Cubouloz, N., Frere, C., 1989. Titan's atmosphere and hypothesized ocean: a reanalysis of the Voyager 1 radio-occultation and IRIS 7.7-μm data. Icarus 79, 328–349.

Lieberman, M.A., Lightenberg, A.J., 1994. Principles of Plasma Discharges and Materials Processing. Wiley, New York. 572 p.

Lindal, G.F., Wood, G.E., Hotz, H.B., Sweetnam, D.N., Eshelman, V.R., Tyler, G.L., 1983. The atmosphere of Titan: an analysis of the Voyager 1 radio-occultation measurements. Icarus 32, 413–430.

Lin-Vien, D., Colthup, N.B., Fateley, W.G., Grasselli, J.G., 1991. The Handbook of Infrared and Raman Characteristic Frequencies of Organic Molecules. Academic Press, San Diego. 503 p.

Maguire, W.C., Hanel, R.A., Jennings, D.E., Kunde, V.G., Samuelson, R.E., 1981. C_3H_8 and C_3H_4 in Titan's atmosphere. Nature 292, 683–686.

Marten, A., Hidayat, T., Biraud, Y., Moreno, R., 2002. New millimeter heterodyne observations of Titan: vertical distributions of nitriles HCN, HC_3N, CH_3CN, and the isotopic ratio $^{15}N/^{14}N$ in its atmosphere. Icarus 158, 532–544.

Mattioda, A.L., Hudgins, D.M., Bauschlicher, J.C.W., Rosi, M., Allamondola, L.J., 2003. Infrared spectroscopy of matrix-isolated polycyclic aromatic compounds and their ions. 6. Polycyclic aromatic nitrogen heterocycles. J. Phys. Chem. A 107, 1486–1498.

McDonald, G.D., Thompson, W.R., Heinrich, M., Khare, B.N., Sagan, C., 1994. Chemical investigation of Titan and Triton tholins. Icarus 108, 137–145.

McKay, C.P., 1996. Elemental composition, solubility, and optical properties of Titan's organic haze. Planet. Space Sci. 44, 741–747.

McKay, C.P., Toon, O.B., 1992. Titan's organic haze. Proceedings. In: Kaldeich, B. (Ed.), Symposium on Titan. ESA SP-338. European Space Agency Publications Divison, Nordwijk, pp. 185–190.

McKay, C.P., Pollcack, J.B., Courtin, R., 1989. The thermal structure of Titan's atmosphere. Icarus 80, 23–53.

McKay, C.P., Pollack, J.B., Courtin, R., 1991. The greenhouse and antigreenhouse effects on Titan. Science 253, 1118–1121.

McKay, C.P., Coustenis, A., Samuelson, R.E., Lemmon, M.T., Lorenz, R.D., Cabane, M., Rannou, P., Drossart, P., 2001. Physical properties of the organic aerosols and clouds on Titan. Planet. Space Sci. 49, 79–99.

O'Donnell, J.H., Sangster, D.F., 1970. Principles of Radiation Chemistry. Edward Arnold, London. 176 p.

Pearse, R.W.B., Gaydon, A.G., 1976. The Identification of Molecular Spectra. Chapman and Hall, London. 407 p.

Podolak, M., Noy, N., Bar-Nun, A., 1979. Photochemical aerosols in Titan's atmosphere. Icarus 40, 193–198.

Rages, K., Pollack, J.B., 1980. Titan aerosols: optical properties and vertical distribution. Icarus 41, 119–130.

Rages, K., Pollack, J.B., 1983. Vertical distribution of scattering hazes in Titan's upper atmosphere. Icarus 55, 50–62.

Ramirez, S.I., Coll, P., da Silva, A., Navarro-Gonzalez, R., Lafait, J., Raulin, F., 2002. Complex refractive index of Titan's aerosol analogues in the 200–900 nm domain. Icarus 156, 515–529.

Rannou, P., Cabane, M., Chassefiere, E., Botet, R., McKay, C.P., Courtin, R., 1995. Titan's geometric albedo: role of the fractal structure of the aerosols. Icarus 118, 355–372.

Rannou, P., Cabane, M., Botet, R., Chassefiere, E., 1997. A new interpretation of scattered light measurements at Titan's limb. J. Geophys. Res. 102, 10997–11013.

Rannou, P., Ferrari, C., Rages, K., Roos-Serote, M., Cabane, M., 2000. Characterization of aerosols in the detached haze layer of Titan. Icarus 147, 267–281.

Rao, C.N.R., 1963. Chemical Applications of Infrared Spectroscopy. Academic Press, New York. 683 p.

Rao, C.N.R., 1975. Ultra-Violet and Visible Spectroscopy. Chemical Applications. Butterworth, London. 242 p.

Ricca, A., Bauschlicher Jr., C.W., Bakes, E.L.O., 2001. A computational study of the mechanisms for the incorporation of a nitrogen atom into polycyclic aromatic hydrocarbons in the Titan haze. Icarus 154, 516–521.

Robertson, J., O'Reilly, E.P., 1987. Electronic and atomic structure of amorphous carbon. Phys. Rev. B 35, 2946–2957.

Rodil, S.E., Ferrari, A.C., Robertson, J., Milne, W.I., 2001. Raman and infrared modes of hydrogenated amorphous carbon nitride. J. Appl. Phys. 89, 5425–5430.

Roth, J.R., 1995. Industrial Plasma Engineering, vol. 1. Principles. Institute of Physics Publishing, Bristol. 538 p.

Roth, J.R., 2001. Industrial Plasma Engineering, vol. 2. Applications to Nonthermal Plasma Processing. Institute of Physics Publishing, Bristol.

Sagan, C., Thompson, W.R., 1984. Production and condensation of organic gases in the atmosphere of Titan. Icarus 59, 133–161.

Sagan, C., Khare, B.N., Lewis, J.S., 1984. Organic matter in the Saturn system. In: Matthews, M.S., Gehrels, T. (Eds.), Saturn. Univ. of Arizona Press, Tucson, pp. 788–807.

Sagan, C., Thompson, W.R., Khare, B.N., 1992. A laboratory for prebiological organic chemistry. Accounts Chem. Res. 25, 286–292.

Sagan, C., Khare, B.N., Thompson, W.R., McDonald, G.D., Wing, M.R., Bada, J.L., Vo-Dinh, T., Arakawa, E.T., 1993. Polycyclic aromatic hydrocarbons in the atmosphere of Titan and Jupiter. Astrophys. J. 414, 399–405.

Samuelson, R.E., Hanel, R.A., Kunde, V.G., Maguire, W.C., 1981. Mean molecular weight and hydrogen abundance of Titan's atmosphere. Nature 292, 688–693.

Scattergood, T., Owen, T., 1977. On the sources of ultraviolet absorption in spectra of Titan and the outer planets. Icarus 30, 780–788.

Scattergood, T.W., Lau, E.Y., Stone, B.M., 1992. 1. Laboratory investigations of shapes, size distributions, and aggregation of particles produced by UV photolysis of model Titan atmosphere. Icarus 99, 98–105.

Smith, B.A., Soderblom, L., Boyce, J., Briggs, G., Bunker, A., Collins, S.A., Hansen, C.J., Johnson, T.V., Mitchell, J.L., Terrile, R.J., Carr, M., Cook II, A.F., Cuzzi, J., Pollack, J.B., Danielson, G.E., Ingersoll, A., Davies, M.E., Hunt, G.E., Masursky, H., Shoemaker, E., Morrison, D., Owen, T., Sagan, C., Veverka, J., Strom, R., Suomi, V.E., 1981. Encounter with Saturn: Voyager 1 imaging science results. Science 212, 163–191.

Smith, B.A., Soderblom, L., Batson, R., Briggs, P., Inge, J., Masursky, H., Shoemaker, E., Beebe, R., Boyce, J., Briggs, G., Bunker, A., Collins, S.A., Hansen, C.J., Johnson, T.V., Mitchell, J.L., Terrile, R.J., Cook II, A.F., Cuzzi, J., Pollack, J.B., Danielson, G.E., Ingersoll, A., Davies, M.E., Hunt, G.E., Morrison, D., Owen, T., Sagan, C., Veverka, J., Strom, R., Suomi, V.E., 1982a. A new look at the Saturn system: the Voyager 2 images. Science 215, 504–537.

Smith, G.R., Strobel, D.F., Broadfoot, A.L., Sandel, B.R., Shemansky, D.E., Holberg, J.B., 1982b. Titan's upper atmosphere: composition and temperature from the EUV solar occultation results. J. Geophys. Res. 87, 1351–1359.

Socrates, G., 2001. Infrared and Raman Characteristic Group Frequencies. Wiley, Chichester. 347 p.

Spinks, J.W.T., Woods, R.J., 1964. An Introduction to Radiation Chemistry. Wiley, New York.

Strobel, D.F., Summers, M.E., Zhu, X., 1992. Titan's upper atmosphere: structure and ultraviolet emissions. Icarus 100, 512–526.

Tamor, M.A., Vassell, W.C., 1994. Raman "fingerprinting" of amorphous carbon films. J. Appl. Phys. 76, 3823–3830.

Tanguy, L., Bezard, B., Marten, A., Gautier, D., Gerard, E., Paubert, G., Lecacheux, A., 1990. The stratospheric profile of HCN on Titan from millimeter observations. Icarus 85, 45–57.

Tauc, J., 1972. Optical properties of non-crystalline solids. In: Abeles, F. (Ed.), Optical Properties of Solids. North-Holland, Amsterdam, pp. 277–313.

Thompson, W.R., Henry, T.J., Schwartz, J.M., Khare, B.N., Sagan, C., 1991. Plasma discharge in $N_2 + CH_4$ at low pressures: experimental results and applications to Titan. Icarus 90, 52–73.

Thompson, W.R., McDonald, G.D., Sagan, C., 1994. The Titan haze revisited: magnetospheric energy sources and quantitative tholin yields. Icarus 112, 376–381.

Toon, O.B., McKay, C.P., Griffith, C.A., Turco, R.P., 1992. A physical model of Titan's aerosols. Icarus 95, 24–53.

Toublanc, D., Parisot, J.P., Brillet, J., Gautier, D., Raulin, F., McKay, C.P., 1995. Photochemical modeling of Titan's atmosphere. Icarus 113, 2–26.

Tran, B.N., Joseph, J.C., Ferris, J.P., Persans, P.D., Chera, J.J., 2003. Simulation of Titan haze formation using a photochemical flow reactor: the optical constants of the polymer. Icarus 165, 379–390.

Vogt, R.E., Chenette, D.L., Cummings, A.C., Garrard, T.L., Stone, E.C., Schardt, A.W., Trainor, J.H., Lal, N., McDonald, F.B., 1981. Energetic charged particles in Saturn's magnetosphere: Voyager 1 results. Science 212, 231–234.

Vogt, R.E., Chenette, D.L., Cummings, A.C., Garrard, T.L., Stone, E.C., Schardt, A.W., Trainor, J.H., Lal, N., McDonald, F.B., 1982. Energetic charged particles in Saturn's magnetosphere: Voyager 2 results. Science 215, 577–582.

Wilson, J.E., 1974. Radiation Chemistry of Monomers, Polymers, and Plastics. Marcel Dekker, New York. 633 p.

Yelle, R.V., Strobell, D.F., Lellouch, E., Gautier, D., 1997. Engineering models for Titan's atmosphere. In: Wilson, A. (Ed.), Huygens, Science, Payload and Mission. ESA SP-1177. European Space Agency Publications Division, Nordwijk, pp. 243–256.

Yung, Y.L., Allen, M., Pinto, J.P., 1984. Photochemistry of the atmosphere of Titan: comparison between model and observations. Astrophys. J. Suppl. 55, 465–506.